

Spring 2018

Geographic Classification of Wines Using Their Elemental and Water Isotopic Composition; Special Emphasis on Washington State, USA

Shirley Orellana
Central Washington University, orellans@cwu.edu

Follow this and additional works at: <https://digitalcommons.cwu.edu/etd>



Part of the [Food Chemistry Commons](#), and the [Viticulture and Oenology Commons](#)

Recommended Citation

Orellana, Shirley, "Geographic Classification of Wines Using Their Elemental and Water Isotopic Composition; Special Emphasis on Washington State, USA" (2018). *All Master's Theses*. 936.
<https://digitalcommons.cwu.edu/etd/936>

This Thesis is brought to you for free and open access by the Master's Theses at ScholarWorks@CWU. It has been accepted for inclusion in All Master's Theses by an authorized administrator of ScholarWorks@CWU. For more information, please contact scholarworks@cwu.edu.

GEOGRAPHIC CLASSIFICATION OF WINES USING THEIR ELEMENTAL AND WATER ISOTOPIC
COMPOSITION; SPECIAL EMPHASIS ON WASHINGTON STATE, USA

A Thesis
Presented to
The Graduate Faculty
Central Washington University

In Partial Fulfillment
of the Requirements for the Degree
Master of Science
Chemistry

by
Shirley Janneth Orellana

May 2018

CENTRAL WASHINGTON UNIVERSITY

Graduate Studies

We hereby approve the thesis of

Shirley Janneth Orellana

Candidate for the degree of Master of Science

APPROVED FOR THE GRADUATE FACULTY

Dr. Anne Johansen, Committee Chair

Dr. Carey Gazis

Dr. Dion Rivera

Dean of Graduate Studies

ABSTRACT

GEOGRAPHIC CLASSIFICATION OF WINES USING THEIR ELEMENTAL AND WATER ISOTOPIC COMPOSITION; SPECIAL EMPHASIS ON WASHINGTON STATE, USA

by

Shirley Janneth Orellana

May 2018

The frequency and scope of wine fraud cases have increased worldwide, leaving wineries vulnerable to damage in reputation and potential lost revenue. In the United States of America, Washington State (WA) is the second-largest premium wine producer where wine fraud could have a significant impact on the industry. In an effort to reduce this risk, advanced analytical instrumentation and statistics were employed to chemically characterize, and thus geographically classify, 118 wines from 4 major wine producing regions located on 3 continents, including 64 wines from WA. Focus was on the analysis of inorganic and chemically stable tracers that are conserved and remain constant in bottled wine: 58 elements and 2 water isotopes, quantified with Inductively Coupled Plasma Mass Spectrometry (ICP-QQQ) and Cavity Ring-Down Spectroscopy, respectively. Linear discriminant analysis resulted in successful regional and continental classification, with 97.5% and 99.2% correct assignments, respectively. WA and California wines were significantly different from each other and from those collected in South America and Europe. The fourteen distinguishing parameters, in order of significance, were silicon, manganese, δD , rhenium, thallium, uranium, zinc, lead, sodium, rubidium, strontium, nickel, cerium and $\delta^{18}O$. Within WA, classification was low for the 7 regions, 6 of which are sub-appellations of one. This study is the first of its kind performed on US wines with

particular focus on WA and represents a solid start for building a larger data base and model that could be used to discriminate between wines worldwide.

TABLE OF CONTENTS

Chapter	Page
I	INTRODUCTION..... 1
	Washington State Wine..... 1
	Wine Fraud 5
	Goals and Objectives..... 6
	Instrumentation 7
	Inductively Coupled Plasma Mass Spectrometry (ICPMS).....7
	Cavity Ring–Down Spectroscopy (CRDS).....12
II	LITERATURE REVIEW 15
	Elemental Composition of Wine Grapes 15
	Stable Water Isotopes in Wine Grapes 17
	Elemental and Stable Isotope Analysis 21
	Argentina..... 22
	Romania 23
	China 25
	South Africa..... 28
	Canada 29
III	JOURNAL ARTICLE–WORLD WINES..... 30
	Abstract 31
	Introduction 32
	Methods 34
	Results and Discussion 36
	Conclusion 54
	Acknowledgements..... 55
	References..... 56
	Supplementary Information..... 57
IV	WASHINGTON STATE WINES 65
	Multielement Analysis..... 65
	Isotope Analysis..... 68
	Geographical Discrimination Analysis..... 71

TABLE OF CONTENTS (CONTINUED)

Chapter		Page
V	CONCLUSION.....	73
	REFERENCES.....	75
	APPENDICES.....	79
	Appendix A–ANOVA results for wines from WA regions.....	79
	Appendix B–PCA factor loadings for wines from WA regions.....	88

LIST OF TABLES

Table		Page
1	California, Washington and National wine grape production in thousands of tons from 2009-2013	2
2	Price per ton for the top five grape varieties in WA from 2013-2014.....	3
3	Top 10 wine exports for Washington State in 2013	4
4	Isotopic composition of red and white wine from two vintage years produced in Napa Valley, CA	20
5	Classification results by region for CA, WA, EU and SA samples	49
6	Variables entered and removed during stepwise method of LDA for World wines	49
7	Standardized canonical discriminant function coefficients for CA, WA, EU and SA wines.	50
8	Classification ability of the LDA model for CA, WA, EU and SA wines.....	50
9	Classification results by continent for NA, SA and EU wines.....	52
10	Standardized canonical discriminant function coefficients for NA, SA and EU wines.....	52
S11	ANOVA results for wines from CA, WA, SA and EU. Significances ≤ 0.05 are marked in green.....	57
S12	PCA factor loadings for wines from CA, WA, SA and EU. Loadings with values ≥ 0.5 are marked in green.....	62

LIST OF FIGURES

Figure		Page
1	Washington State 13 AVAs.	2
2	Total economic impact of wine and related activity production from 2009-2013 in WA State	4
3	An interior system diagram of the 8800 Triple Quadrupole ICPMS showing each main component	7
4	Schematic of nebulizer and spray chamber.....	8
5	Schematic of ICP source.....	8
6	Interface region containing two cones, shadow stop and electrostatic lenses	9
7	Schematic of a quadrupole mass filter	10
8	Schematic of a discrete dynode detector used in the ICPMS system	12
9	Schematic of a CRDS in a Picarro L2130-I Analyzer	13
10	Variation around the world in $\delta^{18}\text{O}$ concentrations.....	18
11	Plot of δD versus $\delta^{18}\text{O}$ of grape juice samples.....	19
12	Isotopic relationship between δD and $\delta^{18}\text{O}$ of water in wine for 2008 (open circles) and 2009 (open square) vintages	21
13	PCA results for Argentinean white wines	22
14	LDA results for Argentinean white wines	23
15	LDA results for Romanian wines	24
16	Relationship between altitude, latitude and $\delta^{18}\text{O}$ for Romanian wines from four different regions.....	25
17	PLS-DA results for Chinese wines from three different regions.....	26
18	Results of LDA by using “enter independents together” method	27

LIST OF FIGURES (CONTINUED)

Figure		Page
19	Results of LDA by using “use step-wise method”	27
20	Discriminant analysis of the two Canadian regions.....	29
21A	Box-and-whisker plots of selected elements in world wines, grouped by regions: CA, WA, SA and EU: Magnesium, Silicon and Sulfur	39
21B	Box-and-whisker plots of selected elements in world wines, grouped by regions: CA, WA, SA and EU: Aluminum, Manganese, Copper and Rubidium	39
22A	Box-and-whisker plots of selected elements in world wines, grouped by regions: CA, WA, SA and EU: Arsenic and Lead	40
22B	Box-and-whisker plots of selected elements in world wines, grouped by regions: CA, WA, SA and EU: Cerium, Samarium, Rhenium and Mercury.....	40
23	Box-and-whisker plot of $\delta^{18}\text{O}$ in world wines, grouped by regions: CA, WA, SA and EU	44
24	Box-and-whisker plot of δD in world wines, grouped by regions: CA, WA, SA and EU	45
25	Plot of δD versus $\delta^{18}\text{O}$ for CA, WA, SA and EU wines	47
26	Classification of CA, WA, EU and SA	51
27	Classification of NA, SA and EU wines	53
28A	Box-and-whisker plots of selected elements in WA wines, grouped by regions WA1 through WA7: Magnesium	67
28B	Box-and-whisker plots of selected elements in WA wines, grouped by regions WA1 through WA7: Silicon.....	67
28C	Box-and-whisker plots of selected elements in WA wines, grouped by regions WA1 through WA7: Aluminum, Manganese and Barium.....	67

LIST OF FIGURES (CONTINUED)

Figure		Page
29	Box-and-whisker plots of selected elements in WA wines, grouped by regions WA1 through WA7: Praseodymium and Gadolinium	68
30	Box-and-whisker plot of $\delta^{18}\text{O}$ in WA wines, grouped by regions WA1 through WA7.....	69
31	Box-and-whisker plot of δD in WA wines, grouped by regions WA1 through WA7.....	70
32	Plot of δD versus $\delta^{18}\text{O}$ for WA wines	71

CHAPTER I

INTRODUCTION

Washington State Wine

Beginning in the 1800s, CA became a domestic source of wine, followed by flourishing in the rest of the U.S. and internationally in the later twentieth century (Cai Community Attributes Inc, 2015). In WA, William Bridgman planted wine grapes in the Yakima Valley in 1914 and in 1933, Dr. Walter J. Clore demonstrated that premium quality wine grapes could be grown in the dry and hot climate of Central and Eastern Washington (Cai Community Attributes Inc, 2015). WA received its first American Viticulture Area (AVA) distinction in 1983, in which a major marketing boon and legal protection became the basis of an additional 12 legal appellations in the coming years (Cai Community Attributes Inc, 2015). AVAs are wine growing regions within the United States that result in unique wines due to their distinguishing geographic, geological and environmental features (Cai Community Attributes Inc, 2015). When an area receives AVA status, this helps the consumer to identify wines within the region and protects the region's market label (Cai Community Attributes Inc, 2015). For the winemaker to specify the appellation on the wine label, once an AVA is established at least 85% of the grapes used in the wine must be from the AVA (Cai Community Attributes Inc, 2015). There are currently 13 different AVAs in WA as shown in Figure 1. WA's first AVA was Yakima Valley being established in 1983 and home to one third of the state's vineyard acreage. Columbia Valley is the state's largest AVA, containing more than 43,000 acres, surpassing all other AVAs in the state.



Figure 1. Washington State 13 AVAs (Cai Community Attributes Inc, 2015).

The production of wine grapes in the state has increased over the past decades. In 1993, there were only 11,000 planted acres, whereas in 2013 that number increased to 50,000 planted acres (Cai Community Attributes Inc, 2015). In 2013, WA produced 210,000 tons of wine grapes and 14.8 million cases of wine (Cai Community Attributes Inc, 2015). It is expected that by 2019, WA wine grape production is to exceed 300,000 tons (Cai Community Attributes Inc, 2015). Nationally, WA State is the second largest premium wine producer, accounting for 4% of the nation’s wine grapes (Cai Community Attributes Inc, 2015). California (CA) is the nation’s leading wine grape producer producing 85% of wine grapes; Table 1 illustrates the difference in tons produced between CA and WA (Cai Community Attributes Inc, 2015).

Table 1. California, Washington and National wine grape production in thousands of tons from 2009-2013 (Cai Community Attributes Inc, 2015).

	2009	2010	2011	2012	2013
California Wine Grape Production	3,703	3,589	3,348	4,018	4,245
Washington Wine Grape Production	156	160	160	188	210
National Wine Grape Production	4,373	4,270	4,534	4,706	5,065

An important factor in determining the total revenue the state receives for grape production is the price per ton (Cai Community Attributes Inc, 2015). In 2014, wine grapes by production value reached \$252 million, where red varieties were valued 40% higher than whites at \$143.8 million (Cai Community Attributes Inc, 2015). It is important to note that WA wine grapes are valued higher than CA wine grapes due to long term contracts with major wineries and WA being primarily a premium rather than bulk wine producer (Cai Community Attributes Inc, 2015). Table 2 shows the average price per ton of the top five grape varietal in WA. By comparison, CA wine grapes on average sold for \$746 per ton for red varieties and \$620 for white varieties in 2013 (Cai Community Attributes Inc, 2015).

Table 2. Price per ton for the top five grape varieties in WA from 2013-2014 (Cai Community Attributes Inc, 2015).

Rank	Varietal	2013	2014
1	Grenache	\$1,914	\$1,674
2	Malbec	\$1,591	\$1,554
3	Petit Verdot	\$1,613	\$1,513
4	Mourvedre	\$1,695	\$1,511
5	Cabernet Franc	\$1,505	\$1,503

The WA wine industry made an estimated \$1.5 billion in sales in 2013, steadily increasing from past years (Cai Community Attributes Inc, 2015). One of the major sources of revenues for wineries is out-of-state sales, generating \$659.9 million in revenue (Cai Community Attributes Inc, 2015). Foreign export of WA wine has also grown in recent years. In 2001, WA received \$4.3 million in foreign sales, a low in comparison to generating \$24.9 million in exports in 2013. Table 3 shows the top 10 wine exports for WA in 2013, where Canada is the largest foreign market for WA, followed by Denmark, Japan and China (Cai Community Attributes Inc, 2015).

Taking into consideration different factors, the impact of wine and grape production has grown over time in WA. The total economic impact of all these factors reached \$4.8 billion in business revenues in 2013, increasing from \$3.5 billion in 2009, as seen by Graph 1 (Cai Community Attributes Inc, 2015). WA’s wine industry ultimately supports \$61.9 million in state taxes (Cai Community Attributes Inc, 2015). With such a large total economic impact, wine fraud could have a significant negative effect on the industry.

Table 3. Top 10 wine exports for Washington State in 2013 (Cai Community Attributes Inc, 2015)

Rank	Country	2013 Sales (mils \$)	Share of Total Export Sales
1	Canada	7.3	29.3%
2	Denmark	2.3	9.4%
3	Japan	2.2	9.0%
4	Germany	1.9	7.7%
5	Finland	1.5	5.9%
6	China	1.2	4.6%
7	Sweden	1.0	4.2%
8	Israel	1.0	4.2%
9	South Korea	1.0	4.1%
10	Switzerland	0.6	2.4%

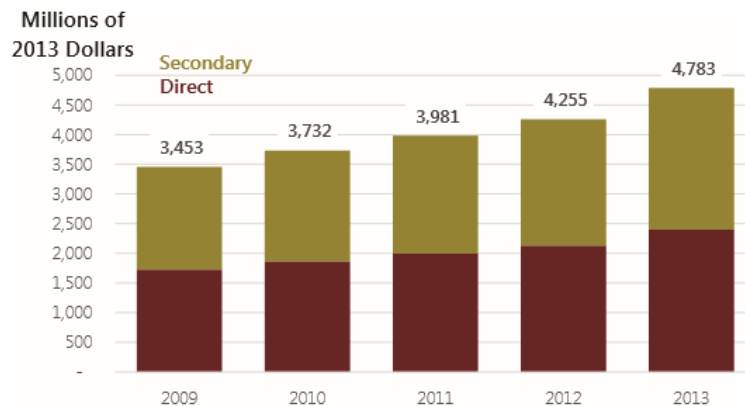


Figure 2. Total economic impact of wine and related activity production from 2009-2013 in WA State (Cai Community Attributes Inc, 2015).

Wine Fraud

To date the largest case in history for wine fraud occurred in 2012 in the state of California. On March 8, 2012, Rudy Kurniawan was arrested by the FBI and in 2013 he was sentenced to 10 years in jail for wine fraud. He had sold over \$20 million of fake wine for more than a decade before being caught (Morgan, 2014). With time, inconsistencies appeared in the wine market, where vintages between 1945 and 1971 from Domaine Ponsot started appearing, yet, the Ponsot family did not start making the wine until 1982 (Cumming, 2016). Around the same time, billionaire Bill Koch found fake bottles in his collection and filed a lawsuit after hiring private investigators, and the FBI got involved. It turns out, that in his own kitchen, he made fake wine by mixing good but not great wine with newer wines, using old bottles and vintage labels. By doing this, he was creating \$1,000 bottles from \$200 bottles and became the first person to be convicted for wine fraud.

Foreign countries are also being impacted by wine fraud. China is a country in which the wine market has grown rapidly (Shen, 2017). The popularity of imported top-end wine has increased making China one of the largest wine consuming countries in the world. The high demand of wine has led to increased counterfeit wines in China (Ambler, 2017). It is estimated, by the Interprofessional Council of Bordeaux Wine, that 30,000 bottles of fake imported wine are sold per hour in China (Ambler, 2017). Chinese food safety researchers conducted a test in which nine samples from wines sold through online and offline channels were tested and two of the bottles bought online contained no grapes whatsoever (Ambler, 2017). In 2017, Shanghai police found 14,000 bottles of fake Penfolds wine being sold through Alibaba's online flea market, which is China's version of Ebay, as well as pubs and karaoke bars (Needham,

2017). Another 2,000 bottles were seized when police arrested five online retailers selling to pubs (Needham, 2017). In March 2018, 12.7 million gallons of falsely labeled Côtes-du-Rhône wine being sold in France (Mustacich, 2018). Approximately 5.3 million gallons of the fake Côtes-du-Rhône were already offered for sale from 2013-2016, investigators also found that 264,000 gallons of fake wine labeled with the prestigious Châteauneuf-du-Pape name was sold during this time (Mustacich, 2018). In an effort to reduce this potential risk of fraud in WA, here we explore the use of advanced analytical techniques to “fingerprint” and build a database of WA wines that could serve to classify each wine to its geographical origin.

Goals and Objectives

The overarching goal of this study is to chemically fingerprint WA wines to set them apart from wines that stem from other regions of the world. To the best of our knowledge, this is the first kind of such study on WA wines. By investigating elemental concentrations and isotopic composition of water, we are building a database that can be used to help reduce the risk of wine fraud in WA. This was accomplished through the following objectives:

Objective 1: Optimize analysis method with state of the art ICP-QQQ by exploiting its high resolution and sensitivity for trace metal analysis as well as major elements.

Objective 2: Optimize H₂O stable isotope analysis technique for wine analysis.

Objective 3: Collect and analyze ~100 wines of which, ~50 WA state wines and ~50 from other major wine producing regions including CA, South America and Europe.

Objective 4: Data will be analyzed with analysis of variance (ANOVA), linear discriminant analysis (LDA) and principal component analysis (PCA).

Instrumentation

Inductively Coupled Plasma Mass Spectrometry (ICPMS)

Due to its multielement analysis capabilities and high sensitivity the most commonly used instrument for the determination of trace elements and “fingerprinting” of food, drinks and wine, is Inductively Coupled Plasma Mass Spectrometry (ICPMS) (Azcarate *et al.*, 2015). An ICPMS functions by combining a mass spectrometer with a high temperature Inductively Coupled Plasma (ICP) source as shown in Figure 3 (Wolf, 2005).

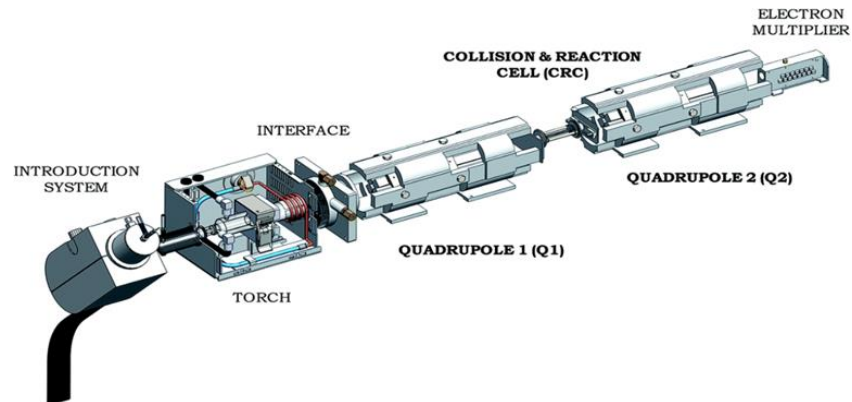


Figure 3. An interior system diagram of the 8800 Triple Quadrupole ICPMS showing each main component (Bolea-Fernandez *et al.*, 2017).

The first step in the ICPMS consists of the pumping of the sample solution into a nebulizer where the sample solution is sprayed into a fine aerosol mist and passed through a spray chamber, as seen in Figure 2. The larger sample droplets get removed by colliding into the spray chamber wall and any excess sample solution remaining is removed by the peristaltic pump drain channel (Agilent Technologies, 2008).

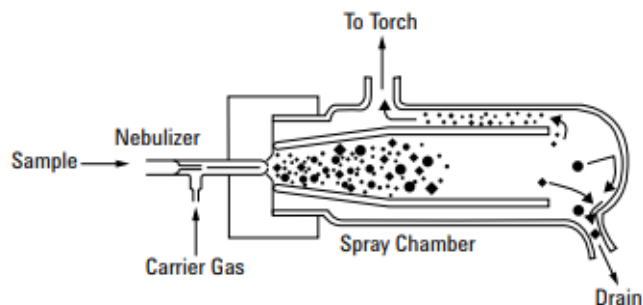


Figure 4. Schematic of nebulizer and spray chamber (Agilent Technologies, 2008).

This aerosol is then carried with argon gas into the ICP, where the argon plasma atomizes and ionizes elements in the sample to form a cloud of positively charged ions. The ICP source consists of three concentric quartz tubes through which argon gas flows through as seen by Figure 5 (Skoog, 2007, 2018). At the top of the tube is a water-cooled induction coil that is powered by a radio frequency generator (Skoog, 2007, 2018). As power is supplied to the load coil, oscillating electric and magnetic fields are established at the end of the torch. A spark applied to the argon gas flowing through the ICP strips electrons off the argon atoms converting them into ions (Skoog, 2007, 2018). These ions then interact with the oscillating fields and collide with other argon atoms creating the plasma or torch, reaching temperatures between 8,000 to 10,000 Kelvin (Skoog, 2007, 2018).

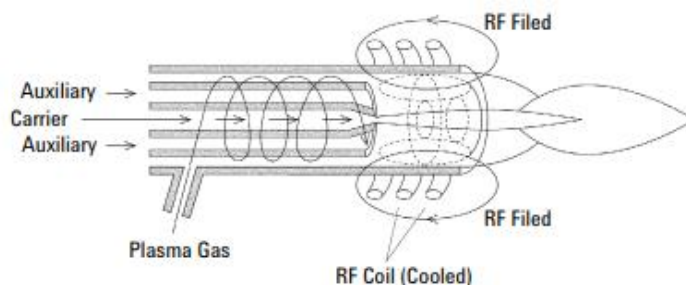


Figure 5. Schematic of ICP source (Agilent Technologies, 2008).

When the elements in the sample are converted to ions by the ICP this allows for the sample

ions to be extracted from the plasma to the vacuum system, which contains a quadrupole mass filter, a collision-reaction cell and another quadrupole mass filter (Wolf, 2005). In order to enter the mass spectrometer, the sample ions need to be transmitted into the low pressure region of the mass spectrometer (Wolf, 2005). The interface region allows for this by creating an intermediate vacuum region using two interface cones, the sample and skimmer cones, observed in Figure 6 (Wolf, 2005). Both cones are metal disks with small slits in the center (Wolf, 2005). The main purpose of these cones is to center the ion beam coming from the ICP torch, a shadow stop is then used to block the photons (Wolf, 2005). Lastly, electrostatic lenses collimate and focus the ion beam from the ICP source into the entrance slit of the mass spectrometer (Wolf, 2005).

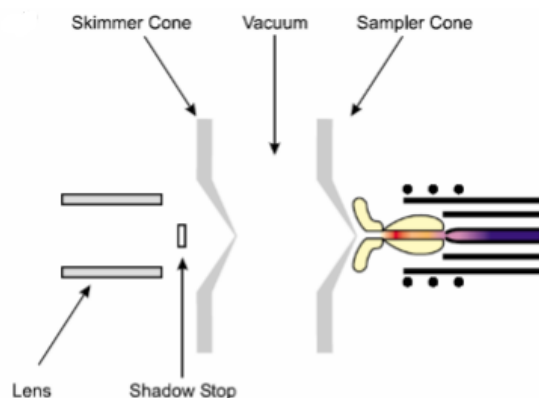


Figure 6. Interface region containing two cones, shadow stop and electrostatic lenses (Wolf, 2005).

The quadrupoles separate the ions by their mass to charge ratio (m/z) using 4 rods, which serve as electrodes, that have alternating AC and DC voltages applied to opposite pairs of the rods, hence the name quadrupole as seen by Figure 7 (Skoog, 2007, 2018). Ions are accelerated into the space between the rods by a potential difference of 5 to 10 V in order to obtain a mass spectrum (Skoog, 2007, 2018). The AC and DC voltages on the rods are simultaneously

increased causing all the ions except those having a certain m/z value to strike the rods and be converted to neutral molecules (Skoog, 2007, 2018). To understand how the quadrupole can filter the ions it is important to consider the effects of the AC and DC voltages being applied. When the positive rods are in the absence of DC voltage, the ions will head towards the center of the channel during the positive half of the AC cycle and will diverge during the negative half (Skoog, 2007, 2018). If an ion strikes the rod during the negative half cycle, the positive charge will be neutralized, and the molecule will be carried out (Skoog, 2007, 2018). When the negative rods are in the absence of AC voltage, the positive ions will attract to the rods (Skoog, 2007, 2018).

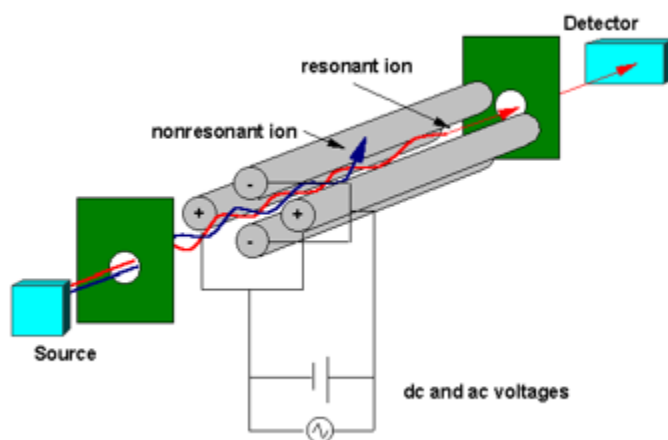


Figure 7. Schematic of a quadrupole mass filter (Tissue, 2000).

The triple quadrupole ICP-MS (ICP-QQQ) consist of a quadrupole 1 (Q1), octopole or collision and reaction cell and another quadrupole (Q2). Q1 has two operation modes utilizing two different scan types; single quad and MS/MS. Single quad is the same as the conventional ICP-MS and is used when no reaction in the cell is expected. When in single quad no gas or He is used and Q1 acts as an ion guide, meaning it just acts as a path for the ions to pass through with no mass filter, whereas Q2 is used as a mass filter. MS/MS mode is specific for ICP-QQQ

where the conventional ICP-MS does not have this feature. MS/MS mode is used when the reaction in the collision and reaction cell is expected and the gases used for this are H₂, O₂ and NH₃ (Agilent Technologies, 2016). When in MS/MS mode both Q1 and Q2 act as mass filters, allowing control of the reactions on the cell. For a typical reaction that can occur in the collision and reaction cell two methods can be used; mass shift and on mass method. An example of a mass shift method includes the elements ⁷⁵As⁺ and ⁴⁰Ar³⁵Cl⁺, both having a mass to charge ratio (m/z) of 75. Q1 can be set to m/z of 75 but both of these ions will pass through, so O₂ gas is used in the collision and reaction cell. Arsenic reacts with the oxygen to produce an oxide having m/z of 91 (⁷⁵As¹⁶O⁺). The argon chloride ion does not react with oxygen so no change will occur on this ion. This will then allow to set Q2 to m/z 90 allowing the arsenic oxide to pass through to the detector, filtering out the argon chloride. An example of on mass method can be explained with ⁸⁰Se⁺ and ⁴⁰Ar⁴⁰Ar⁺, both having m/z of 80. Q1 is set to m/z 80 observing no filter of the unwanted ion. This leads to using H₂ gas to prevent the interference of these two ions. Interference is prevented by reaction of the argon dimer with the H₂ gas, producing a hydride changing the m/z of the argon dimer to 41 (⁴⁰Ar¹H⁺). By setting Q2 to m/z 80, ⁸⁰Se⁺ can pass through to the detector while argon hydride is filtered out. By using the reaction cell double charged, oxide, isobaric ions and polyatomic ions interferences are reduced (Agilent Technologies, 2016).

Finally, as the ions get separated by their m/z ratio, the ions that were able to go through the quadrupole then enter the detector, which is a dynode detector as seen in Figure 8. The detector allows the positive ions to be converted into an electrical signal (Skoog, 2007, 2018). It does this by holding each dynode to a higher voltage, so as the ions strike the surfaces

of the dynodes, electrons are emitted (Skoog, 2007, 2018). This allows for a cascade of electrons because the electrons are attracted to the next dynode down the chain. As the electrons reach the last dynode, there is a large number of electrons for every ion that strikes the cathode (Skoog, 2007, 2018). The detector counts the discrete hits of a particular m/z ion which are then compared to a set of standards of known concentrations to determine concentrations (Agilent Technologies, 2016).

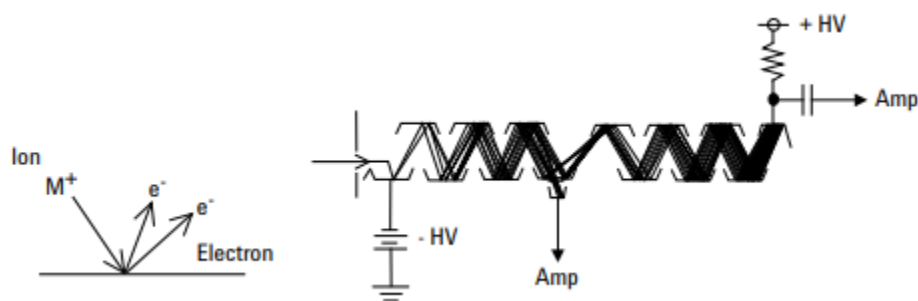


Figure 8. Schematic of a discrete dynode detector used in the ICPMS system (Agilent Technologies, 2008).

Cavity Ring-Down Spectroscopy (CRDS)

Another technique used to “fingerprint” wines is the analysis of water isotopes. A popular isotopic water analyzer for delta oxygen 18 ($\delta^{18}\text{O}$) and delta deuterium (δD) is the Picarro L2130-I Analyzer. The Picarro analyzer uses cavity ring-down spectroscopy (CRDS) to measure stable isotopes in water. CRDS functions by using the infrared absorption spectrum of gas phase molecules to measure the concentration of water isotopes. The CRDS in a Picarro analyzer uses a single-frequency laser diode beam in which it enters a cavity having three reflectivity mirrors, as shown in Figure 9. The three mirrors in the cavity allow for a continuous traveling light wave, providing excellent signal to noise in comparison to a two-mirror cavity that only allows a standing wave. The cavity rapidly fills with circulating laser light when the

laser is on and a photodetector senses the small amount of light leaking through one of the mirrors. This leak of light allows for production of a signal that is directly proportional to the intensity inside the cavity. When the threshold of the photodetector is reached, the laser is abruptly turned off but the light already within the cavity still bounces between the mirrors. The mirrors have slightly less than 100% reflectivity, because of this the light intensity inside of the cavity gradually leaks out and exponentially decays to zero. This decay is what is called “ring down” and is measured by the photodetector. The reflectivity of the mirrors is what determines the amount of time it takes for the ring down to occur (Picarro Inc., 2016).

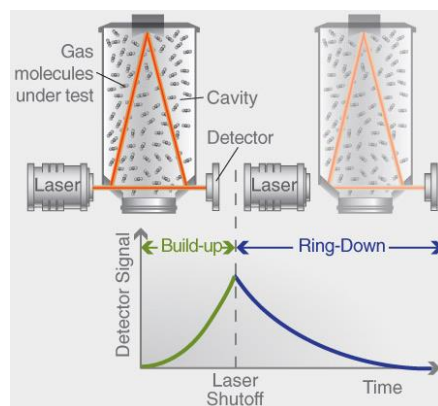


Figure 9. Schematic of a CRDS in a Picarro L2130-I Analyzer (Picarro Inc., 2016).

When a gas species is introduced into the cavity a second loss mechanism within the cavity occurs because the gas species absorbs the laser light. This absorption accelerates the ring down time compared to a cavity without a gas species being introduced to the cavity. The Picarro ultimately calculates and compares the ring down time of the cavity with an absorbing gas and without an absorbing gas. This is accomplished by using a laser whose wavelengths can be tuned rather than removing the gas from the cavity. In doing so, the laser can be tuned to different wavelengths where the gas does not absorb light and to wavelengths where the gas does absorb light. Now, the “cavity only” ring down time can be compared to the ring down

time when the gas is absorbing the light and causing optical loss in the cavity. A continuously repeated measurement of the ring down time is collected at several different wavelengths as the laser is adjusted to the molecular signature of the analyte gas. This allows the ring down profile to be transformed into an absorption curve with a lineshape. Determination of the isotope ratio is achieved by a multiparameter fit to the lineshape and is proportional to the area under the curve (Picarro Inc., 2016).

CHAPTER II

LITERATURE REVIEW

Wine is a complex system containing mainly water, sugar, and alcohol in addition to inorganic and organic compounds that impact its main characteristics (Jakubowski et al., 1999). The majority of abundant mineral elements found in wine originate from the grape itself through absorption from the soils where the grapes are grown (Cheng et al., 2015). Logically, a difference in individual concentration and elemental profile of the soil can thus be observed from different geographical origins (Cheng et al., 2015). There are many factors that may affect the element uptake by plants, which include age, root depth, soil pH, rainfall and temperature of the region (Greenough et al., 1997). During the winemaking process, elements are not modified or metabolized, allowing mineral elements to be considered as good indicators of the wine's geographical region (Cheng et al., 2015).

Elemental Composition in Wine Grapes

The primary source of trace elements for plants and humans is soil (Hooda, 2010). The most significant trace elements in the environment for human/animal health are metals that include: cadmium, chromium, cobalt, copper, gold, lead, manganese, mercury, molybdenum, nickel, palladium, platinum, rhodium, silver, thallium, tin, vanadium and zinc (Hooda, 2010). Though chlorine and iron are not considered trace elements, because they are found in soils and plants at greater concentrations than 100 mg kg^{-1} , they are still necessary in plant life processes as well for animals or humans, making them essential micronutrients (Hooda, 2010).

The main anthropogenic sources of trace elements to soil include: atmospheric deposition, land application of sewage sludge and animal manure, land disposal of industrial

coproducts and waste, and fertilizers, lime and pesticides used in agriculture (Hooda, 2010).

Hooda (2010) also reported that the single largest source of non-soil derived trace metals to soils in the 1980s was through atmospheric deposition, accounting for 50-80% of its contribution. Major reductions in atmospheric emissions have been achieved but it remains a main source of trace metal input to soils (Hooda, 2010).

The total metal input of grapes to wine is mainly influenced by natural sources (Cozzolino, 2015). The concentrations of these metals are influenced by grape maturity, type of grape, type of soil in the vineyard and the climatic conditions during grape growth (Cozzolino, 2015). A secondary contributor is the external contamination added during growth or different stages of winemaking. Contamination during grape growth and development comes from environmental pollution, fertilizer and plant protection application, or directly from the soil. Application of pesticides, fungicides and fertilizers during the growth period of the grapes increases concentrations of elements such as arsenic, cadmium, copper, manganese, lead and zinc. Thus, during the wine making process, increased concentrations of these elements in the juice can occur due to the long contact time between wine and the materials (iron, copper, and zinc) comprising the winemaking machinery parts.

Elements playing a relevant role in winemaking include zinc, essential at low concentrations for the correct development of alcoholic fermentation. Copper, iron and manganese have organoleptic effects contributing to the haze and taste of wines (Cozzolino, 2015). Iron is found in substantial quantities depending on several factors, the most important of which is derived from the soil through: (1) the grape berry being covered by dust or (2) absorption by the plant through the roots (Cozzolino, 2015). Stabilization problems in wine can

occur when there are excessive amounts of iron since it can be oxidized to a ferric form causing precipitation of pigmented materials or with orthophosphate ions (Cozzolino, 2015).

The origin of copper has been associated with copper-based vineyard sprays (Cozzolino, 2015). In wines, copper may be of exogenous or endogenous origin, where most exogenous copper is due to copper sulfate used for spraying the vines to prevent mildew (Cozzolino, 2015). As a fungicide, sodium arsenite is employed in viticulture to prevent a grapevine necrotic disease called eutypa dieback. It has also been shown that treatment with different fungicides like mancozeb, zoxamine and copper oxychloride increases the concentrations of manganese, zinc, copper, lead and cadmium of wines and grapes. Arsenic levels in wines mainly depend on soil composition, climatic conditions, grape variety, uses of pesticides, winemaking technology and storage conditions. Concentrations of lead is a consequence of the deposition of airborne particulate matter on grapes or uptake from groundwater by the grapevine or soil. Lead can also be released from bronze tanks, taps, pumps and tubing containers used in winemaking.

Stable Water Isotopes in Wine Grapes

The isotopic composition of the water of wine depends on the environment in which it originates, both natural and anthropogenic (Raco et al., 2015). Across the earth, water varies greatly due to the variable climatic patterns and strong trends are observed with increases in latitude and altitude as seen in Figure 10 (Raco et al., 2015).

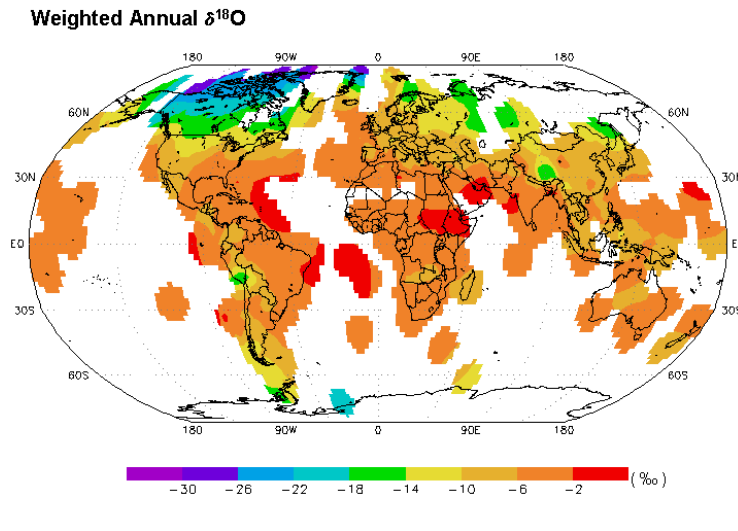


Figure 10. Variation around the world in $\delta^{18}\text{O}$ concentrations (International Atomic Energy Agency, 2001).

Water isotopes are reported as delta values, expressed as fractions in per mil (‰) (Iannone et al., 2010). These values are calculated using the following formula:

$$\delta = \left[\frac{R_{\text{sample}} - R_{\text{standard}}}{R_{\text{standard}}} \right]$$

where R can be defined to be the ratio $[\text{H}^2]/[\text{H}^1]$ or $[\text{O}^{18}]/[\text{O}^{16}]$ in the sample and standard (Iannone et al., 2010). Note that these ratios comprise of the rare isotope to the most abundant isotope. The accepted standard is known as Vienna Standard Mean Ocean Water (VSMOW) and has a ratio of 0‰ (Iannone et al., 2010). Climatic conditions of a location control evaporation and transpiration, which further fractionates the water compared to the ground water by causing enrichment in delta deuterium (δD) and delta oxygen-18 ($\delta^{18}\text{O}$) in surface water and in leaves and fruit casing (Raco et al., 2015). The combination of oxygen and hydrogen isotope composition of water of wine has become a powerful tool to discriminate wines from different regions and has been further combined with other tools.

In a study performed on the $\delta^{18}\text{O}$ and δD concentrations of various sections of grape plants found that heavy hydrogen and oxygen isotopes are enriched due to evapotranspiration (Dunbar, 1983). The enrichment in the leaves was the highest but there was also enrichment in the fruit itself (Dunbar, 1983). This led the authors to also measure $\delta^{18}\text{O}$ and δD of grape juices and the results can be seen in Figure 11 (Dunbar, 1983). The experimental line in the figure for the grape juices falls between the meteoric line and the evaporation line in which the authors concluded that the physical process causing the enrichment was evapotranspiration (Dunbar, 1983).

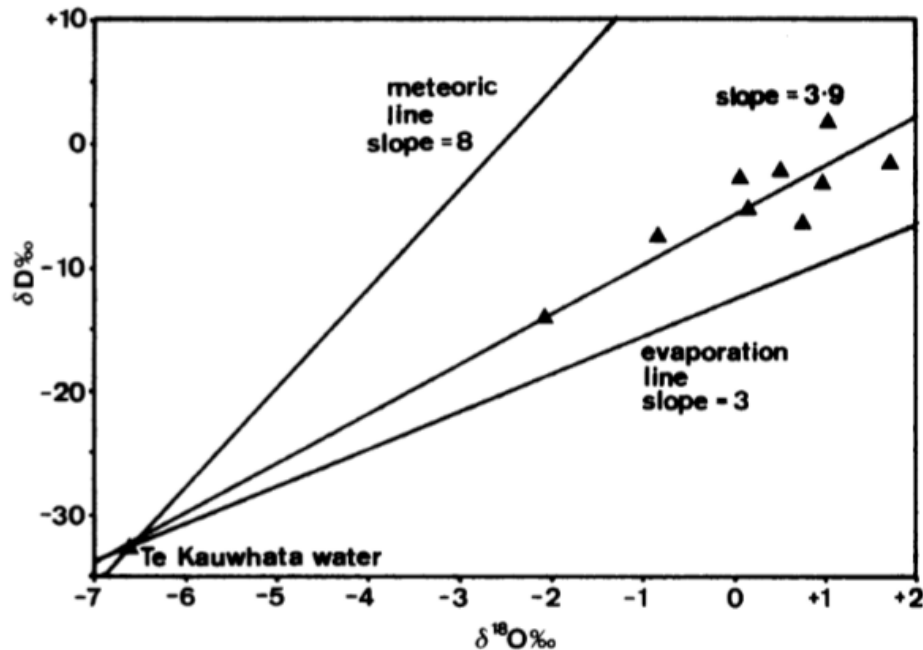


Figure 11. Plot of δD versus $\delta^{18}\text{O}$ of grape juice samples (Dunbar, 1983).

During berry development in grape plants, the berry integrates the local meteoric water from recent precipitation throughout the growing season in which the wine made from these berries can perhaps show the stable isotopic composition of precipitation for that year (Ingraham, 1999). Grape berries are affected by temperature and relative humidity, as they

mature and approach harvest, which control the grade of evapotranspiration within the plant (Ingraham, 1999). This can ultimately somewhat cover the isotopic composition of the source water but temperatures and precipitations vary in different regions of the world which would sequentially give different isotopic composition for different regions (Ingraham, 1999). Previous studies have shown that wines that are produced in warmer, drier climates are isotopically different from wines produced in colder, wetter climates (Ingraham, 1999). The effects of weather are ultimately more important than source water on the isotopic composition of wine (Ingraham, 1999). An example of this is the analysis carried out for white wines in comparison to red wines produced in the same vintage year where white wines showed to be 4 ‰ more depleted in $\delta^{18}\text{O}$ values than red wines (Ingraham, 1999). Results are seen in Table 4 and are justified by the additional maturation and transpiration that occurred for the red wine grape berries as a result of these berries being harvested 3 weeks after the white wine berries (Ingraham, 1999).

Table 4. Isotopic composition of red and white wine from two vintage years produced in Napa Valley, CA (Ingraham, 1999).

Variety	Year	$\delta^{18}\text{O}$	δD
Cabernet Sauvignon	1991a	+8.1	+11
Cabernet Sauvignon	1991b	+8.0	+11
Grey Riesling	1991a	+4.1	+0
Grey Riesling	1991b	+4.1	+3
Cabernet Sauvignon	1992a	+10.0	+20
Cabernet Sauvignon	1992b	+10.2	+19
Grey Riesling	1992a	+5.5	+7
Grey Riesling	1992b	+5.4	+3

In a study on the classification of three groups of countries' isotopic ratios of wines in terms of climatic variables associated with two extreme climates, discriminant analysis shows that the three sets of countries were well assigned into the extreme climate groups. The extreme climate groups included: cold humid, hot-dry or both cold humid and hot-dry regions (Martin et

al., 1988). Different vintage years also show important differences between δD and $\delta^{18}O$ due to climate factors (Raco et al., 2015). Figure 12 displays the relationship between δD and $\delta^{18}O$ of water in wine and year of production from 2008 to 2009 (Raco et al., 2015).

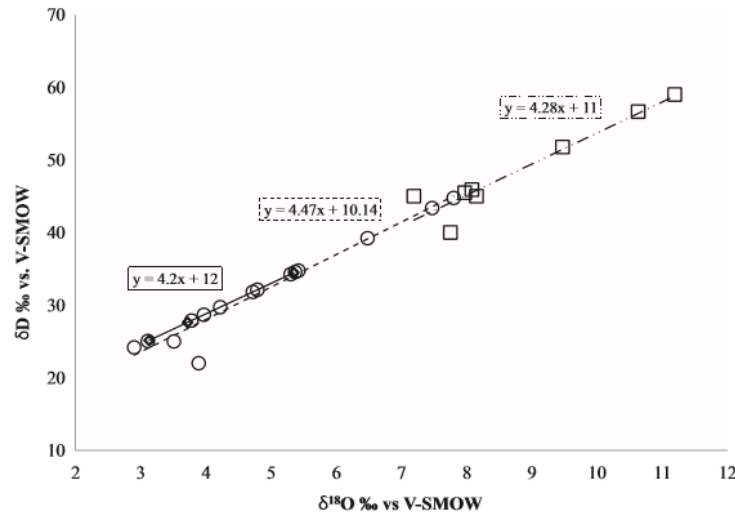


Figure 12. Isotopic relationship between δD and $\delta^{18}O$ of water in wine for 2008 (open circles) and 2009 (open square) vintages (Raco et al., 2015).

A shift in $\delta^{18}O$ can be observed in which the values from 2009 are more positive and values from 2008 are more negative (Raco et al., 2015). These values are caused from hot and dry to cold and humid climatic conditions during the harvest of these grapes (Raco et al., 2015).

Favorable conditions during harvest were observed in 2009, in which there was reduced rainfall and increased temperatures whereas in 2008 there were unfavorable climatic conditions (Raco et al., 2015). In this case, the time of harvest is a critical factor due to climatic conditions where even lowering the temperature by 1 °C can considerably change the isotopic value by 3-5 ‰ (Raco et al., 2015).

Elemental and Stable Isotope Analysis

Many scientists around the world have been investigating the classification of wine via ICPMS for multielement determination of wine in combination with stable isotope analysis and

have had successful results. Following are research results to discriminate wines from different regions with elemental concentrations and isotopic composition reported by country.

Argentina

In Argentina, researchers developed a method for determining elements in 57 white wines by ICPMS and chemometric pattern-recognition techniques (Azcarate et al., 2015).

Principal component analysis was used to visualize groups in the Argentinean white wines.

Results are displayed in Figure 13 and displays two principal components (PC) that explained 95.95% of the variance in data.

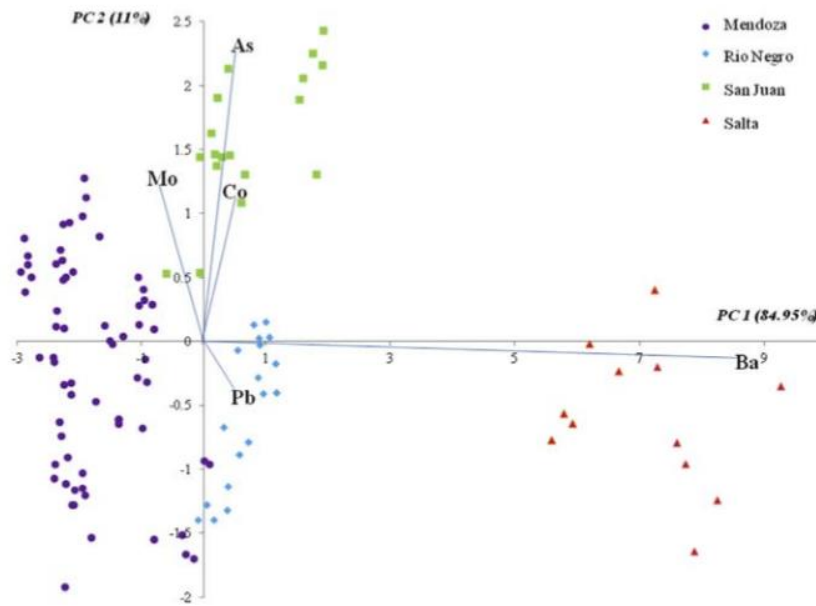


Figure 13. PCA results for Argentinean white wines (Azcarate et al., 2015).

The plot also shows which variable had more weight for each plane, in which PC1 is mainly associated positively to Ba separating wines from Salta and also uses Pb allowing discrimination between Mendoza and Rio Negro (Azcarate et al., 2015). PC2 used As, Mo and Co in order to discriminate the wines from San Juan (Azcarate et al., 2015). By linear discriminate analysis the researchers were able to correctly discriminate the four geographical regions being evaluated

using the five ultratrace elements given in PCA that included: Ba, As, Pb, Mo and Co (Azcarate et al., 2015). Results from LDA are presented in Figure 15, reaching discrimination rates higher than 96% for prediction and validation data sets (Azcarate et al., 2015). Only four samples were not classified correctly, represented with a red star in Figure 14, and the authors suggest that it is possible these samples correspond to a different origin not stated on the label (Azcarate et al., 2015). With these results, the researchers concluded that this is a trustworthy technique to validate the geographical origin, authenticity and quality control of wines (Azcarate et al., 2015).

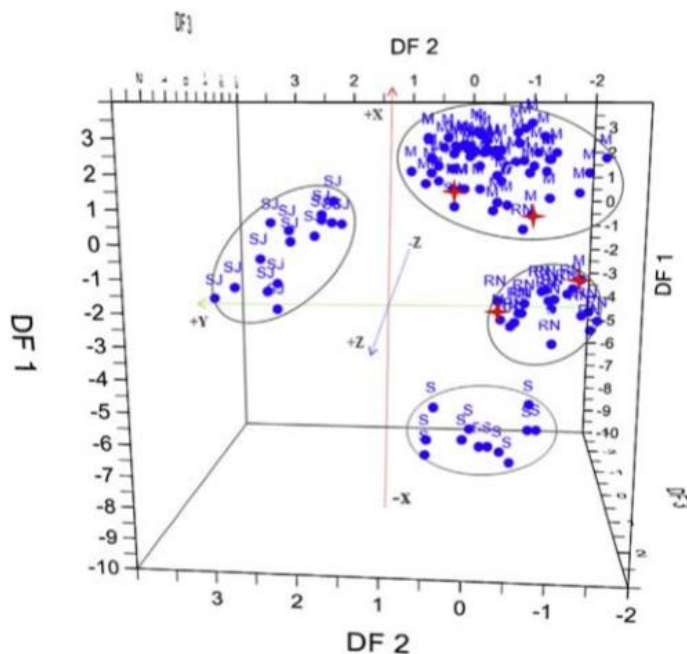


Figure 14. LDA results for Argentinean white wines (Azcarate et al., 2015).

Romania

In Romania, four major vineyards, during vintages 2009 and 2010, were investigated in order to classify the wines to their geographical origin through isotopic and elemental fingerprinting (Dinca et al., 2016). LDA was used to process the data using values for C and O stable isotope ratios and ten trace elements; results are illustrated in Figure 15 (Dinca et al.,

2016). The authors found that function 1 in LDA represented 71.85% of the variance providing the main separation and correlating it with Mn, Cu, Sr and V (Dinca et al., 2016). Function 2 represented 18.53% of the variance and was correlated with $\delta^{13}\text{C}$, $\delta^{18}\text{O}$ and Pb allowing for discrimination of the Iasi region (Dinca et al., 2016). LDA allowed the authors to classify a total of 90.37% of the wines and also verified the influence of vintage year (Dinca et al., 2016).

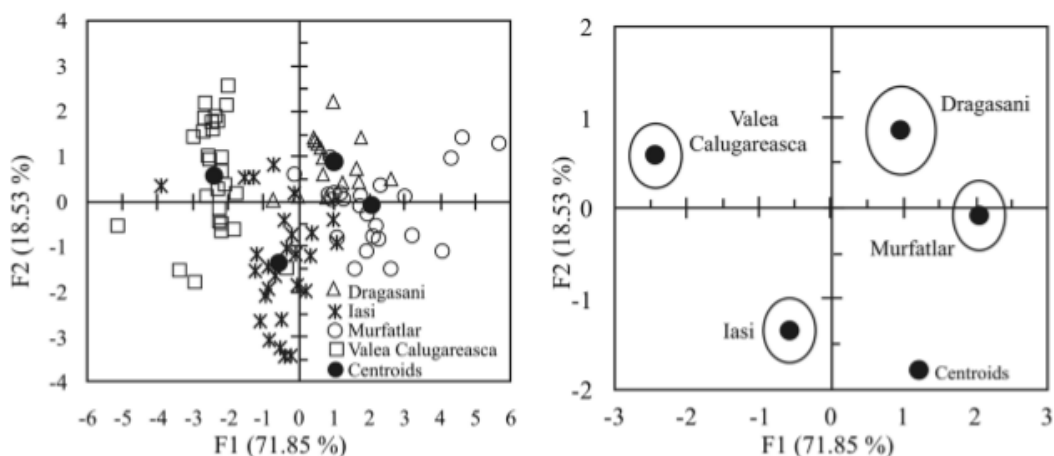


Figure 15. LDA results for Romanian wines (Dinca et al., 2016).

The authors also found $\delta^{18}\text{O}$ to be a suitable indicator to discriminate the wines being analyzed to their geographical region and had the strongest relationship with the climatic conditions (Dinca et al., 2016). The vineyards of Dragasani and Valea Calugareasca had higher average values of $\delta^{18}\text{O}$ when compared to those from Murfatlar and Iasi (Dinca et al., 2016). This is explained by the climatic conditions for each region as well as elevation effects as seen in Figure 16 (Dinca et al., 2016). Although the figure does not show a strong connection between altitude and $\delta^{18}\text{O}$, authors observe that the lowest value for $\delta^{18}\text{O}$ is seen in the more elevated regions (Dinca et al., 2016). With these results, the authors concluded that the most suitable indicators to discriminate between regions were Mn, Ni, Cu, Zn, Pb, V and $\delta^{18}\text{O}$ highlighting successful differentiation of wines (Dinca et al., 2016).

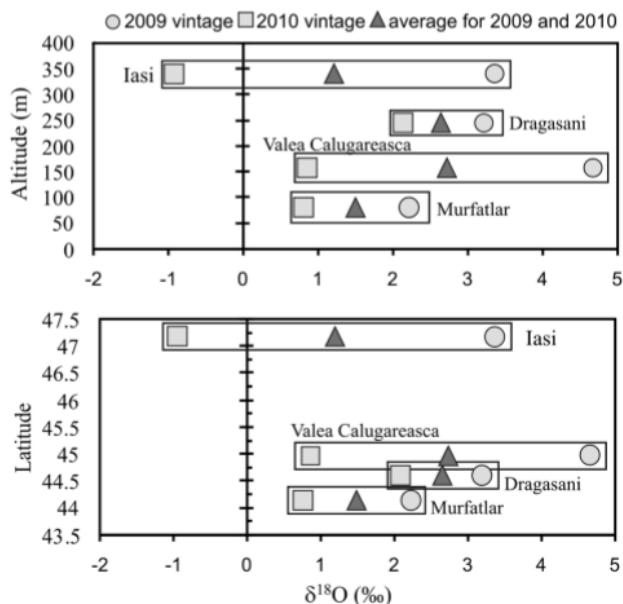


Figure 16. Relationship between altitude, latitude and $\delta^{18}\text{O}$ for Romanian wines from four different regions (Dinca et al., 2016).

China

The elemental profile and oxygen isotope ratio for Chinese wines from Changji, Mile and Changli were analyzed using ICPMS, inductively coupled plasma optical emission spectroscopy and isotope ratio mass spectrometry (Fan et al., 2017). Data was first analyzed using ANOVA to obtain the elements having the most significance for the discrimination of the three regions (Fan et al., 2017). ANOVA identified the key elements to be Ca, Al, Mg, B, Fe, K, Rb, Mn, Na, P, Co, Ga, As, Sr and $\delta^{18}\text{O}$. These elements were then used as inputs for partial least squares discrimination analysis (PLS-DA) and support vector machine analysis (SVM) (Fan et al., 2017). Figure 17 shows the results for PLS-DA in which X-variate 1 and X-variate 2 accounted for 49% of the total variance in the raw data (Fan et al., 2017). This allowed for the distinction between the three regions (Fan et al., 2017). A cross validation and random data splitting with a training and testing set ratio of 70:30 was performed, the average correct classification of the training set for PLS-DA and SVM models were both 98% (Fan et al., 2017). The values for the test set for

PLS-DA and SVM were 95% and 97%, respectively (Fan et al., 2017). The authors concluded that the combination of $\delta^{18}\text{O}$ and elemental profile is a solid approach to verify the geographical origin of these Chinese wines (Fan et al., 2017).

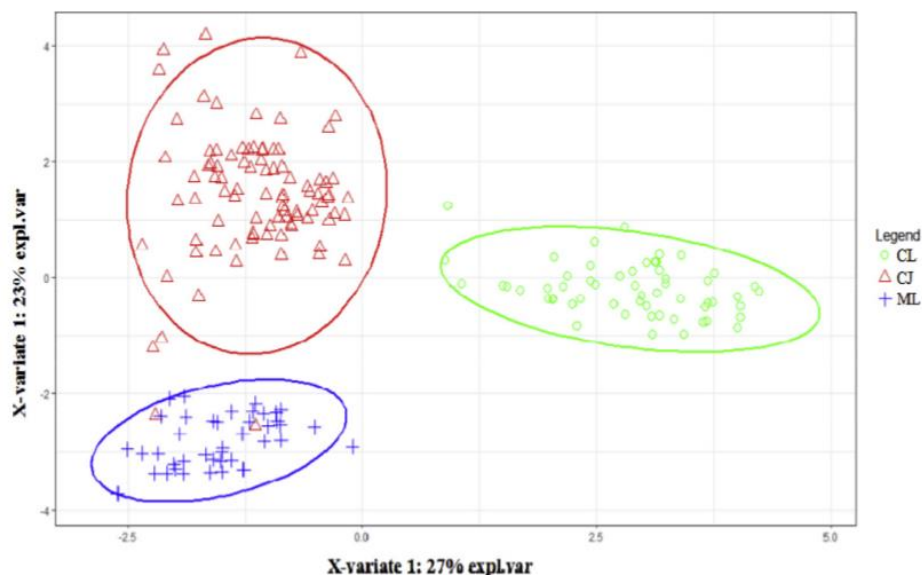


Figure 17. PLS-DA results for Chinese wines from three different regions (Fan et al., 2017).

A second study was also able to distinguish wines from Pengali, Yinchuan and Changli, three districts in China, with four general macro-elements K, Ca, Na and Mg and four micro-elements Fe, Zn, Sr and Mn (Cheng et al., 2015). Concentration of each element was determined by inductively coupled plasma-atomic emission spectroscopy (Cheng et al., 2015). PCA extracted three principal components and PC1 and PC2 clearly separated Yinchuan wines from Penglai and Changli (Cheng et al., 2015). Discriminant analysis was also evaluated to discriminate the data by using both “enter independents together” and “use step-wise method” (Cheng et al., 2014). In the first method “enter independents together” all eight elements were used to discriminate all three regions with 100% accuracy, as be seen in Figure 18 (Cheng et al., 2015). A cross validation was performed and 95.8% of the samples were correctly classified with only two samples being misclassified (Cheng et al., 2015). In the second method “use

step-wise method” only three types of elements (Sr, Mn and K) were used to discriminate the three regions (Cheng et al., 2015). Figure 19 displays results of this method and indicates that all three regions were correctly classified by 100% (Cheng et al., 2015). When performing cross validation for this method, 100% of the samples were also correctly classified (Cheng et al., 2015). The authors determined that “use step-wise method” was optimal for analysis due to the results of the cross-validation methods (Cheng et al., 2015).

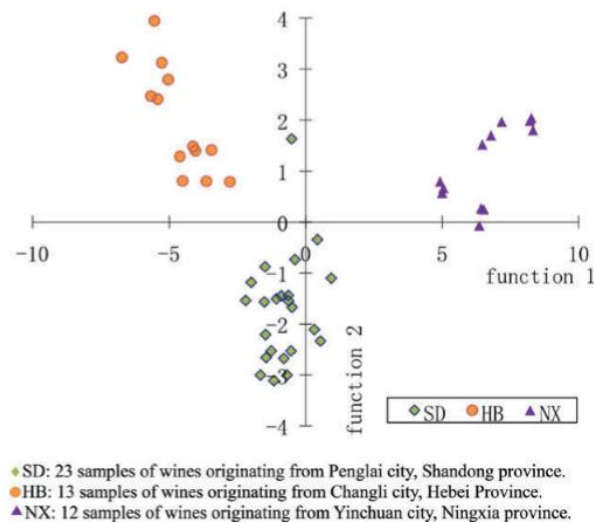


Figure 18. Results of LDA by using “enter independents together” method (Cheng et al., 2015).

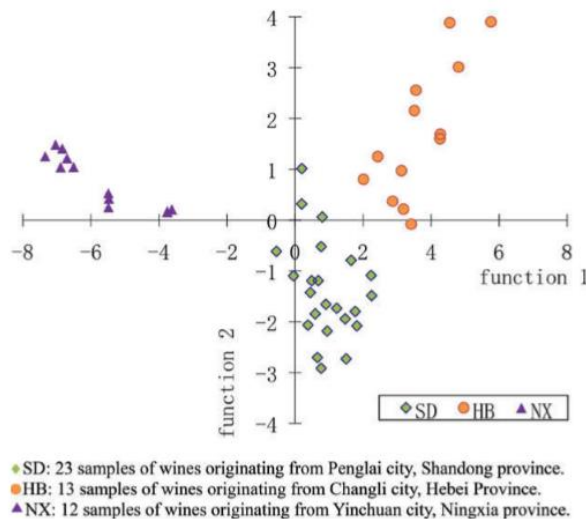


Figure 19. Results of LDA by using “step-wise method” (Cheng et al., 2015).

South Africa

In South Africa, wines from the producing regions of Stellenbosch, Robertson and Swartland were analyzed by ICPMS (Coetzee et al., 2005). A total of 40 elements were analyzed by multivariate statistical analysis and of these 40 only 20 elements (Li, B, Mg, Al, Si, Cl, Sc, Mn, Ni, Ga, Se, Rb, Sr, Nb, Cs, Ba, La, W, Tl and U) showed differences amongst the three regions (Coetzee et al., 2005). LDA further differentiated between the dependent variables, correctly classifying the wines to each region by 100% using Al, Mn, Rb, Ba, W and Tl and in the training set and cross validation (Coetzee et al., 2005). Further analysis was conducted for the elements Al, Sc, Mn, Ni, Ga, Se, Ru, Sr, Cs, Ba, W and Tl using PCA (Coetzee et al., 2005). Three principal components were identified explaining 74.3% of the variability in the data in which PC1 explained 40.6%, PC2 24.7% and PC3 9% (Coetzee et al., 2005). The component scores of PC1 and PC2 clearly discriminated the three regions as well as the red and white wines within each region (Coetzee et al., 2005).

Another study carried out in South Africa demonstrated successful classification of wines in a single wine South African district called Stellenbosch (Coetzee et al., 2014). Classification of these wines was possible by use of ICPMS as an accurate elemental data system and multivariate statistical analysis based on combining cluster analysis, principal component analysis and discriminant analysis (Coetzee et al., 2014). It was determined that suitable indicators for these regions included the elements B, Ba, Cs, Cu, Mg, Rb, Sr, Tl and Zn (Coetzee et al., 2014).

Canada

Canadian wines from the Okanagan Valley and Niagara Peninsula were analyzed with ICPMS and multivariate analysis to achieve discrimination of the two regions (Taylor et al., 2003). Of the 34 elements analyzed by ICPMS only 10 discriminated the two regions with 100% accuracy in the multivariate analysis (Taylor et al., 2003). In Figure 20, wines were plotted according to the discriminant function obtained using the 10 elements: U, V, Al, Sb, Co, Zn, Sr, Rb, Mo and Mn (Taylor et al., 2003).

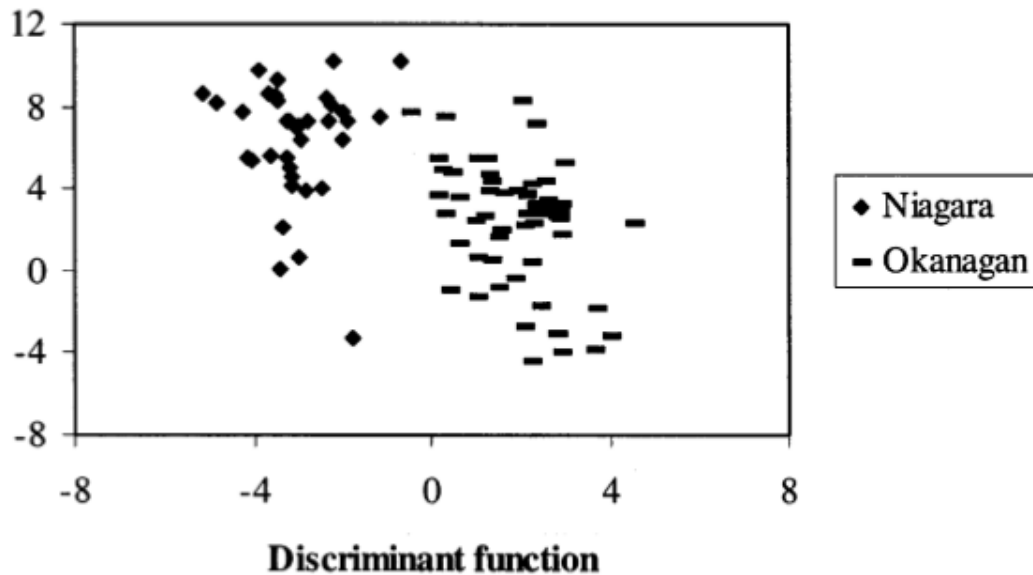


Figure 20. Discriminant analysis of the two Canadian regions (Taylor et al., 2003). Further investigation was conducted by analysis of vineyard soil samples from the Okanagan and Niagara regions (Taylor et al., 2003). The regions were discriminated particularly with the alkaline earth elements Mg, Ca, Sr and Ba in which higher concentrations could be observed in the Okanagan soil samples (Taylor et al., 2003). A comparison between Sr concentrations in wine and soil indicated differences suggesting that there is an influence of soil but other factors also affect the concentration in the wine (Taylor et al., 2003).

CHAPTER III

JOURNAL ARTICLE-WORLD WINES

GEOGRAPHIC CLASSIFICATION OF WINES USING THEIR ELEMENTAL AND WATER ISOTOPIC COMPOSITION

Shirley Orellana, Anne M. Johansen, and Carey Gazis

Department of Chemistry, Central Washington University, Ellensburg, WA 98926

ABSTRACT

The frequency and scope of wine fraud cases have increased worldwide, leaving wineries vulnerable to damage in reputation and potential lost revenue. In the United States of America, Washington State (WA) is the second-largest premium wine producer where wine fraud could have a significant impact on the industry. In an effort to reduce this risk, advanced analytical instrumentation and statistical methods were employed to chemically characterize and geographically classify 118 wines from 4 major wine producing regions located on 3 continents, including 64 wines from WA. Focus was on the analysis of inorganic, chemically stable tracers that are conserved and remain constant in bottled wine. To this end, 58 elements and 2 water isotopes were quantified with Inductively Coupled Plasma Mass Spectrometry and Cavity Ring-Down Spectroscopy, respectively. Linear Discriminant Analysis resulted in successful regional and continental classification, with 97.5% and 99.2% correct assignments, respectively. WA and California wines were significantly different from each other and from those collected in South America and Europe. The fourteen distinguishing parameters, in order of significance, were silicon, manganese, δD , rhenium, thallium, uranium, zinc, lead, sodium, rubidium, strontium, nickel, cerium and $\delta^{18}O$. This study is the first of its kind to focus on WA wines and represents a solid start for building a larger data base and model that could be used to discriminate between wines worldwide.

INTRODUCTION

The state of Washington (WA) has become the second largest premium wine producer in the United States (US) (Cai Community Attributes Inc, 2015). In 2013, WA produced 210,000 tons of wine grapes and 14.8 million cases of wine, receiving \$236.2 million in wine grape sales and \$2.4 billion in direct and secondary wine related revenues (Cai Community Attributes Inc, 2015). WA's wine industry also had a \$4.8 billion economic impact in business profits and supported \$61.9 million in state taxes (Cai Community Attributes Inc, 2015). With such a large total economic impact, wine fraud could have a significant negative effect on the industry. In an effort to reduce this potential risk of fraud in WA, here we explore the use of advanced analytical techniques to "fingerprint" WA wines, classifying each wine to its geographical origin and comparing chemical signatures with those from wines produced in other regions of the world. Currently, 13 different American Viticulture Area's (AVA) are registered in WA (Figure 22). WA's first AVA was Yakima Valley being established in 1983 and home to one third of the state's vineyard acreage. Columbia Valley is the state's largest AVA containing more than 43,000 acres surpassing all other AVAs in the state.

Due to its multielement analysis and high sensitivity, Inductively Coupled Plasma Mass Spectrometry (ICPMS) is currently one of the most used techniques for the determination of trace elements and "fingerprinting" of wine (Azcarate et al., 2015). Many scientists around the world have been investigating the classification of wine via ICPMS and have had successful results. In a study in Argentina, researchers used ICPMS and linear discriminate analysis (LDA) to correctly discriminate the four geographical regions being evaluated with only five elements that included: Ba, As, Pb, Mo and Co (Azcarate et al., 2015). They were able to reach

discrimination rates higher than 96% for prediction and validation data sets, deeming this technique trustworthy in validating the geographical origin, authenticity and quality control of wines. Another study carried out in South Africa demonstrated successful classification of wines in a single wine district called Stellenbosch (Coetzee et al., 2014). Classification of these wines was possible by use of ICPMS and multivariate statistical analysis based on combining cluster analysis, principal component analysis and discriminant analysis. Suitable indicators for these regions included the elements B, Ba, Cs, Cu, Mg, Rb, Sr, Tl and Zn. In the present study, an Inductively Coupled Plasma Triple Quadrupole Mass Spectrometer (ICP-QQQ) was used to quantify 66 elements at sub parts-per-billion (ppb) levels.

Stable isotopes of H₂O are another excellent classifier to further constrain the geographic origin of wine due to climate diversity (Dutra et al., 2011). In a study in Brazil, $\delta^{18}\text{O}$ in wine water was efficient in differentiating the 3 regions studied, even though there was no statistical difference amongst the varieties (Dutra et al., 2011). Scientists in Romania also found $\delta^{18}\text{O}$ to be a suitable indicator to discriminate wines to their geographical region and to display the strongest relationship with climatic conditions (Dinca et al., 2016). Using LDA with values for C and O stable isotope ratios and concentrations of 10 trace metals, 90.37% classification of the Romanian wines and verification of vintage year were achieved (Dinca et al., 2016).

The overarching goal of this study is to chemically characterize WA wines to set them apart from wines that stem from other regions of the world. This will be accomplished by determining elemental compositions and isotopic ratios in conjunction with statistical analyses. Through this effort, we start building a database and model that will help detect wine fraud of WA wines. To the best of our knowledge, this will be the first study of this kind for wines from

WA and placed in relation to other major wine producing regions in the world.

METHODS

Sample Collection and Preparation. Wine samples were collected between 2016 and 2017 from local wineries and bottled wines. For sample collection, 20-mL amber glass vials with Teflon lined caps were prepared by acid cleaning in 5% nitric acid to reduce contaminants. The vials were first triply rinsed with nanopure water, placed in the 5% nitric acid bath, fully submerged in the acid by applying a lid, leaving no air space between the vials and lid and left soaking for 24 hours. Thereafter, vials were triply rinsed with nanopure water, transferred to a water bath containing nanopure water, left soaking for another 24 hours and then triply rinsed with nanopure water again before storage filled to the top with nanopure water until use. Cleaning of vials took place in a class 100 clean laboratory. This procedure proved necessary to reduce background contaminant levels.

To fill the vial with wine, the vial was emptied, rinsed three times with small aliquots of the wine of interest, and filled with the sample leaving no airspace. Before analysis, a 2.00 mL aliquot of wine was filtered through with a 0.2 μm pore-sized syringe filter, into a new acid cleaned amber glass vial. To achieve a tested adequate dilution of 1:20, 1.00 mL of the filtered wine was mixed with nanopure water containing 1% HNO_3 and 0.5% HCl . This sample was prepared in an acid cleaned HDPE test tube for direct analysis on the ICP-QQQ (Collins, 2015).

ICP-QQQ Analysis. For analysis with ICP-QQQ an internal standard (ISTD) and a series of mixed calibration standards were prepared. The ISTD corrects for signal drift and enhances the signal for certain elements. The ISTD was made by diluting 50.0 μL of the concentrated internal

standard mixture containing 100 µg/mL (100 ppm) of Bi, Ge, In, Li⁶, Lu, Rh, Sc and Tb, to a final volume of 50.0 mL, resulting in a 1 ppm ISTD working solution. The dilution included 8.0 mL of methanol, 0.5 mL HNO₃, 50.0 µL of Triton-X, and nanopure water to make a total of 50.0 mL. The final solution contained 1% HNO₃, 16% methanol and traces of Triton-X. The ISTD mixes automatically with the sample before sample introduction at 1/16 of the flowrate of the sample, thus the final methanol concentration in the sample was around 1%. This background carbon supplied by methanol has shown to selectively double the signals of elements with high ionization potential, including As, Se, Te, and P, while the surfactant Triton-X leads to a better flow of solution into the system due to increased surface tension (Emmett Soffey, from Agilent). Calibration standards containing 1% HNO₃ and 0.5% HCl were made by serial dilution of a combination of 4 separate mixed standards that together contained 66 elements. The Collision/Reaction cell (CRC), was used to resolve spectral interferences using of He and H₂ gases for the collision mode (Sugiyama et al., 2014). The choice of gas depended on the type interference, where He and H₂ gases were effectively used for polyatomic ion interferences by use of Kinetic Energy Discrimination (KED) (Sugiyama et al., 2014). Examples of interferences that were removed were 40Ar⁺ on 40Ca⁺, 40Ar⁺ 16O⁺ on 56Fe⁺ and 40Ar²⁺ on 80Se⁺ (Sugiyama et al., 2014).

Picarro Analysis. Isotopic analysis of water in wine was measured with Picarro L2130-i by use of the Picarro Induction Module (IM), which extracts water from the samples. Samples were prepared by placing a hole-punched sized filter paper into a tri-folded metal strip. Then, 3 µL of filtered wine was injected onto the filter paper and inserted into a vial to be introduced to the IM. The wine sample was introduced 6 times using the same filter paper and the first 2 data

points were discarded because of memory effects and the rest of the data points were averaged. The filter paper was changed for every new wine sample.

Statistical Analysis. One-way analysis of variance (ANOVA), principal component analysis (PCA) and linear discriminant analysis (LDA) were performed on SPSS software (ver. 24.0, IBM). ANOVA and PCA provided important information regarding each variable and their significance in the large data sets. After running ANOVA, Tukey's test was run finding which specific group means were significantly different from each other. LDA was essential in maximizing the separability among known categories by determining the best-fit parameters for classification of the samples and selecting the combination that showed the least number of classification errors.

RESULTS AND DISCUSSION

Data Preparation and Organization

Before statistical analyses were performed, elements for which 50% or more of the samples fell below the detection limit (BDL) were removed from further analyses. This was the case for 4 out of the 62 elements and included chromium, niobium, ruthenium and tellurium. All remaining BDL entries were replaced with zeros. Elements for which more than 25% of the samples were replaced with zeros included beryllium, platinum, gallium and selenium, and coincidentally none of these elements emanated as significant descriptors in the analyses described below. ANOVA, PCA and LDA were performed on the 58 elements and Delta O-18 ($\delta^{18}\text{O}$) and Delta D (δD). This group, denoted as "world wines", included 118 samples which were geographically categorized into 4 regions: Washington State (WA, N=64), California State

(CA, N=16), Europe (EU, N=26) and South America (SA, N=12). Of these 118 samples, 101 were red wines and 17 were white wines, latter of which all came from WA. EU wines stemmed from 5 different countries and SA wines from 2. Results are presented starting with an overview and discussion of region means, medians, and standard deviations of statistically most significant components in each of the four world regions. In this step the intent is to reduce data and visualize trends. In short, outputs from ANOVA, PCA and LDA were inspected in combination to identify components that maximized inter-regional differences and were representative of the various PCs. Many of these components naturally emanated as significant in all three analyses. Elements are presented and discussed first, followed by water isotopes. Focus is then on the LDA outputs that most effectively discriminated regions from each other.

World Wines Multielement Analysis

For the world wines, 15 most significant components were chosen for visualization and discussion. Concentrations of 13 elements are shown in box-and-whisker plots in Figures 21 and 22 and the additional 2 components with significant roles, i.e. the water isotopes, are plotted and discussed in the subsequent section. Outliers were omitted from the plots as these skewed the y-axis making the graphs difficult to read. Means, medians and error bars remained unchanged, however, which is the reason for medians and means to be very different at times, such as seen for magnesium in Figure 21A. Elements are grouped in figures by their concentration ranges, with elements in Figures 21A and 21B having higher concentrations than those in Figures 22A and 22B. Horizontal lines above or below the box-and-whiskers indicate significant differences between two regions as determined with ANOVA and Tukey's test, with one star representing a p -value less than 0.05 and two stars a p -value of less than 0.001. In

addition, the middle row at the bottom of each plot notes whether the element was significant in (i) the PCA (i.e., factor loadings of more than 0.5) and if so, in which PC it appeared, and/or (ii) LDA.

Of the higher concentration elements, magnesium, silicon, aluminum, manganese and rubidium are considered to be soil derived, entering the grape through root uptake. In this dataset, as indicated in Figures 21A and 21B, each of these elements appears in different PCs implying that each is independent of the others despite the fact that they are all soil derived. Aluminum appears in PC1, accounting for 17.5% of the variance, while rubidium and manganese are in PC2, with 9.8% of the variance (see Supplementary Information Table 12 for more detail). Silicon in PC7 (4.2% variance) correlates with thorium and uranium. Magnesium correlates with other major cations including potassium and calcium in PC4 (5.3% variance). Tukey's test reveals that in particular silicon and rubidium show significant inter-regional variability as indicated by the 5 horizontal bars stretching across the various data pairs and the fact that both are significant in the LDA. Note that there are 6 comparison pairs for the 4 regions. These results for rubidium are consistent with what is seen in literature. For instance, in South African wines, rubidium, averaging between 176 to 630 ppb, resulted as a good discriminator between 23 estates from the Stellenbosch wine district (Coetzee et al., 2014).

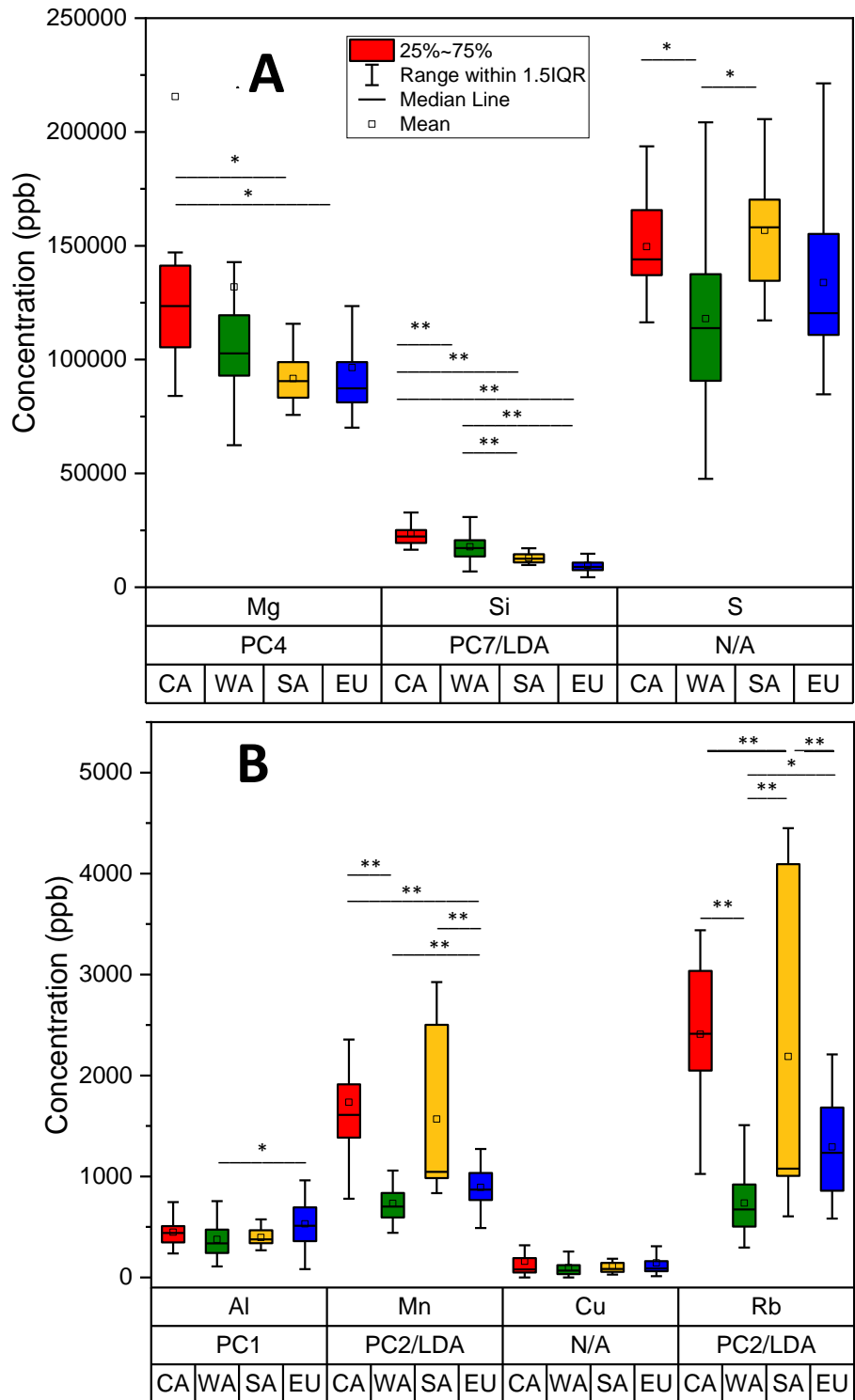


Figure 21. Box-and-whisker plots of selected elements in world wines, grouped by regions: CA, WA, SA and EU: **A.** Magnesium, silicon and sulfur and **B.** Aluminum, manganese, copper and rubidium.

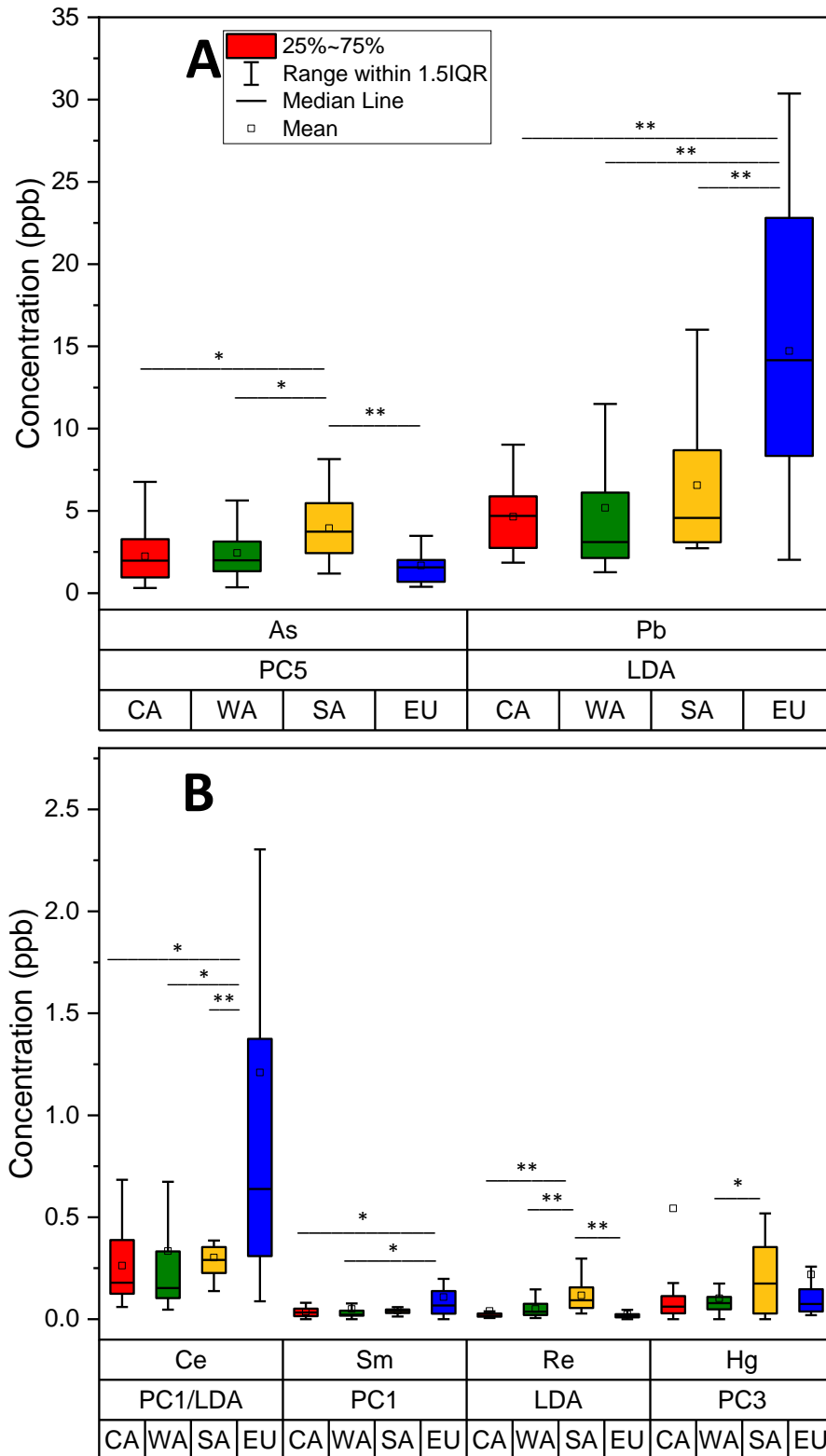


Figure 22. Box-and-whisker plots of selected elements in world wines, grouped by regions: CA, WA, SA and EU: **A.** Arsenic and lead and **B.** Cerium, samarium, rhenium and mercury.

Wines from two regions in Canada, the Okanagan Valley and Niagara Peninsula, noted mean rubidium values of 446 ppb and 680 ppb, and it being one of 10 elements to discriminate between regions (Taylor et al., 2003). Interestingly, except for the WA wines, rubidium concentrations in the rest of our tested samples exceeded those reported in mentioned studies. Manganese tracks rubidium, as seen in the pattern of concentrations and in the fact that both manganese and rubidium appear in PC2. This observation seems sensible in the context of the limited literature on manganese in wines and that manganese also is assimilated through the roots and thus depends on soil and environmental conditions.

Sulfur and copper are elements associated with the winemaking process as they are added to treat wines in the forms of sulfur dioxide and copper sulfate. Sulfur dioxide is used to protect wine from oxidation and microbial spoilage during storage, whereas copper sulfate is used to treat sulfur-off odors in wine. It is seen here that WA wines have significantly lower sulfur concentrations compared to CA and SA wines. This is consistent with observations made in a previous study performed in collaboration with Amy Mumma (CWU World Wine Program) and Holly Pinkart (CWU Biology) on WA Cabernet Sauvignons (Mumma et al., 2010). Because sulfur dioxide (SO₂) is an irritant and can be harmful to sensitive consumers, legal limits exist for total SO₂ concentrations. In the US, this limit is 350 mg/L, as SO₂, which translates into 175.2 mg/L (ppm) as S ($= 350\text{mg SO}_2/\text{L} \times (32.07 \text{ g S/mol}) / 64.07 \text{ g SO}_2/\text{mol}$). In Europe this limit is set at 100 ppm as S for red wines. Thus, while CA and WA wines fall below the US legal limit, more than half of the EU wines exceed the EU standard. The legal limit for total SO₂ in South America is 250 mg/L, i.e., 125.1 ppm as S, which is not met by a significant number of samples. Copper shows no significant differences between the regions or proved to be important in the PC and

LDA, however, due to its increased use in copper vessels it was included here for viewing.

Of the less abundant elements, arsenic, lead, and mercury (Figures 22A and 22B) are considered to be anthropogenically derived from the deposition of ambient aerosol particles and from the application of pesticides, fungicides and fertilizer. Arsenic (in PC5, variance 5.1%) was significantly higher in SA wines compared to all other areas, however, all concentrations fell below the EPA drinking water standard of 10 ppb. Arsenic is known to stem from past application of pesticides and naturally occurring minerals in the soil. Lead and mercury stem primarily from their particulate emission of fossil fuel combustion. Lead in EU wine samples displayed significantly higher concentrations compared to the other regions, with approximately half the samples exceeding the EPA drinking water standard of 15 ppb. Mercury can be emitted from coal combustion and during precious metal extraction. Mercury appears in PC3 (5.5% variance) together with other heavy metals. These heavy metals are used as catalysts in the electronic industry and for high temperature applications. Due to their strong correlations and relatively higher concentrations in SA samples they are likely reaching the grapes through emissions from precious metal extraction processes and are thus associated with mining activities possibly from Brazil through Minas Gerais and Argentina's Sierra de Cordoba.

The least abundant elements of significant impact, cerium and samarium (Figure 22B), are considered rare-earth elements (REE) and are likely derived from soils as they appear in PC1 with aluminum. Cerium in EU wines is significantly higher compared to the other three regions and appears in the LDA as significant. Finally, rhenium (Figure 22B) is another low concentration element that emanates as important, yet it does not correlate with any of the

extracted PCs. Although not much information can be found on this element, it seems to be naturally derived and significantly most abundant in the SA wine samples.

World Wines Isotope Analysis

For the water isotopes, as seen in Figures 23 and 24, 5 comparison pairs are significantly different for $\delta^{18}\text{O}$ and 4 for δD . They appear in the same PC, correlating with the rubidium/manganese soil components mentioned earlier (i.e., PC2, 9.8% of variance, see Supplementary Information Table 14 for more detail). CA wines have higher $\delta^{18}\text{O}$ and δD ratios compared to WA and SA wines, indicating that the wines are enriched in the heavier isotopes. WA wines have the lowest $\delta^{18}\text{O}$ and δD ratios, being enriched in the lighter isotopes. World wine isotopes range from -4.75 to 19.95 ‰ for $\delta^{18}\text{O}$ and -65.9 to 53.2 ‰ for δD and are plotted against each other in Figure 25. This figure includes the Global Meteoric Water Line (GMWL) which describes precipitation data around the globe with a slope of 8. Precipitation waters get lighter moving from the equator toward the poles along this line, and a deviation toward lower slopes is typical after evaporative losses such as are typical for surface waters. Across the earth, water varies greatly due to the variable climatic patterns and strong negative trends are observed with increases in latitude and altitude (Raco et al., 2015). Wine samples from WA have water isotope ratios for both $\delta^{18}\text{O}$ and δD that are significantly lighter, whereas wines from CA are significantly heavier compared to all other regions. In general terms, this is consistent with the GMWL in that higher latitude waters are lighter than lower latitude waters.

Our observations are consistent with what other studies have shown. For instance, wines from the south region of Brazil, considered as a temperate area, had lower $\delta^{18}\text{O}$ values

than wines of warmer counties (Dutra et al., 2011). Average values found in the three temperate Brazilian regions: Serra Gaucha (0.05‰), Serra do Sudeste (2.28‰) and Campanha (1.29‰) were consistently lower than the average for the warmer regions (5.2‰). WA wine $\delta^{18}\text{O}$ are consistent with those found in the temperate regions of Brazil, while the values from EU and SA are more in line with the warmer regions of Brazil (Dutra et al., 2011). The same was seen for Romanian wines from the wet and cold climate region of Iasi where the $\delta^{18}\text{O}$ value was -2.19‰ (Dinca et al., 2016).

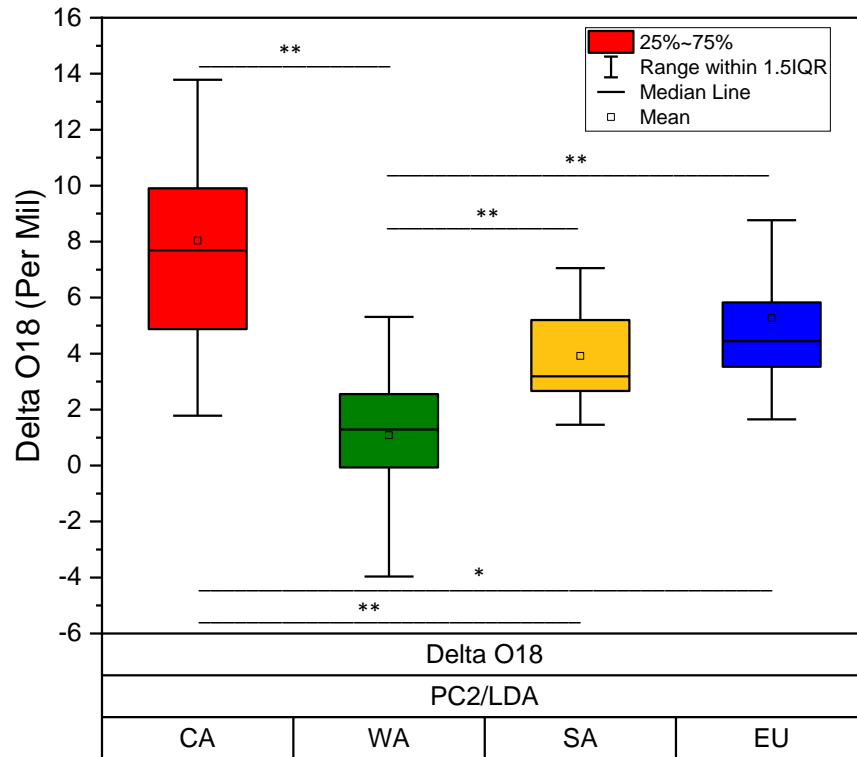


Figure 23. Box-and-whisker plot of $\delta^{18}\text{O}$ in world wines, grouped by regions: CA, WA, SA and EU.

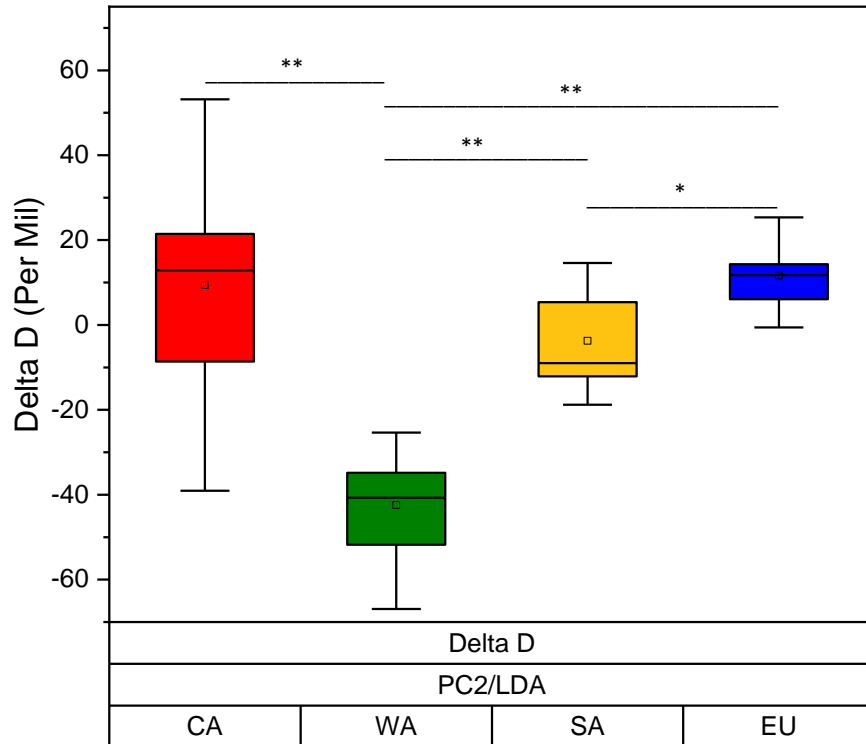


Figure 24. Box-and-whisker plot of δD in world wines, grouped by regions: CA, WA, SA and EU.

As seen in Figure 25, all samples lay below the Global Meteoric Water Line (GWML), which is expected due to enrichment in heavier hydrogen and oxygen isotopes because of the fractionation during evapotranspiration (Dunbar, 1983). Evapotranspiration is the sum of the loss of water from the ground surface into the atmosphere and the transpiration of plants. Throughout maturation the grape berry's evapotranspiration is affected by temperature and relative humidity (Ingraham, 1999). This process modifies the isotopic composition of the source water and leads to a shallower line, i.e., smaller slope, in the δD versus $\delta^{18}O$ plot. It is interesting to note that the slopes for CA and WA wines are similar at around 4.6, which correspond to the local evaporative losses (LEL) observed in lakes and soils in the US (Gibson et al., 2008). Slopes for EU and SA wines are significantly smaller and larger, 2.3 and 5.4,

respectively. Even after omission of the one seeming outlier (from Italy) at the upper end of the line for EU samples in Figure 25, the slope increased only to 2.8. Low slope numbers in the range of 2-3 have been associated with soil waters in regions where surface waters are associated with slopes of 4-5, such as in South America, Africa, Australia and Europe (Gibson et al., 2008). Thus, since wines in the EU are dry farmed, i.e., depend on soil and precipitation waters, a slope between 2 and 3 is reasonable. CA, WA and SA vineyards, on the other hand, are presumably watered with surface waters, which would result in a signature closer to that of the irrigation water. Grape juices from New Zealand have reported slopes of 3.9 (Dunbar et al., 1983), which falls between the GMWL and evaporation line (slope=3) in which the authors indicated the physical process causing the enrichment of the water in grapes is probably evaporation, i.e. evapotranspiration (Dunbar et al., 1983). The slope of evaporation lines depends on information of precipitation and atmospheric moisture as well as relative humidity and temperature (Gibson et al., 2008).

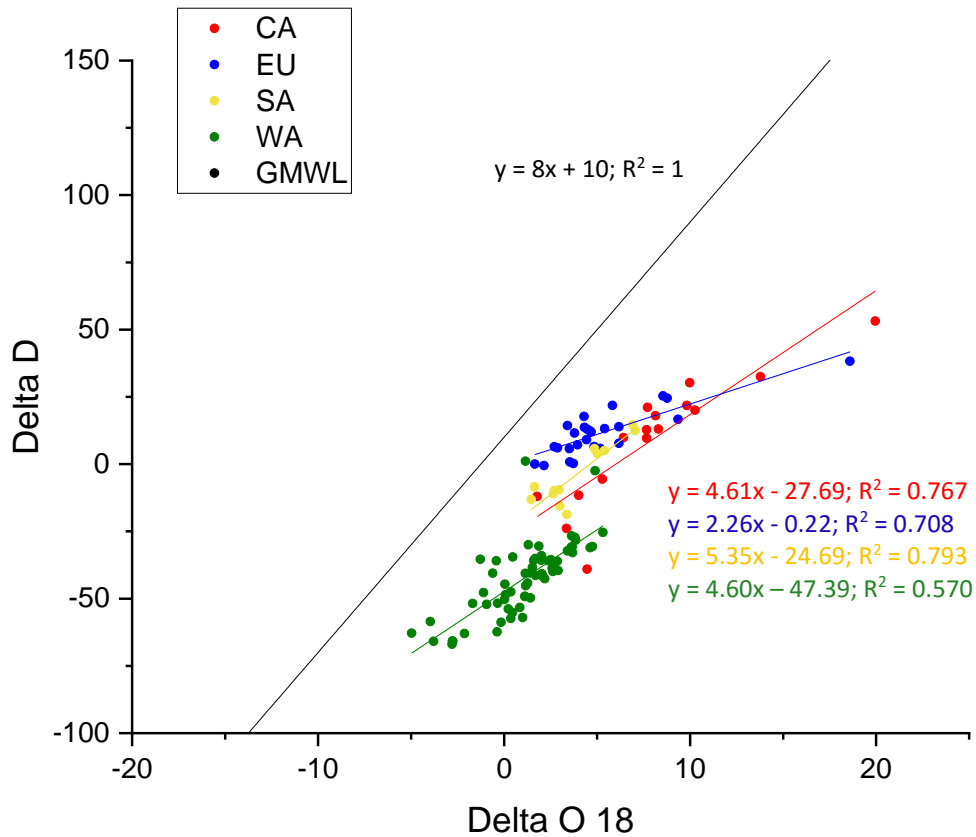


Figure 25. Plot of δD versus $\delta^{18}O$ for CA, WA, SA and EU wines.

Word Wines Geographical Discrimination Analysis

LDA was used to discriminate between wines geographically. By determining the best-fit parameters for classification of the samples it maximizes the separability among known categories, and it has been applied widely for classification of wines elsewhere (Azcarate *et al.*, 2015). In the stepwise method used here, the model starts with no variables, then at each step it enters the variable with the highest impact into the model. Any variables with no impact are left out in the last step and no more are added to the model. For the LDA analysis including all samples and assigning the 4 indicated regions, 14 components resulted as most significant. These are listed in Table 6 in order of how they were selected in the stepwise method. Similar

elements appearing as key components in PCA and visualized in Figure 23A, 23B and 24B, are also important discriminators in LDA, including silicon, manganese, δD , rubidium and cerium. All outputs of LDA, except uranium, also show significance in ANOVA. The model resulted in 97.5% correct assignment of samples to their respective region using the 14 components in 3 functions for which standardized canonical discriminant function coefficients are listed in Table 7. Figure 26 depicts the separation amongst wines from CA, WA, SA and EU defined by three discriminant functions. Boxed points are the three wine samples that were falsely classified. Two of these samples are from WA's Columbia Valley, one of which was classified as CA (1998 Columbia Valley wine) and the other as EU (2013 Columbia Valley wine). In addition, the CA sample that was incorrectly classified as WA was from Healdsburg and happened to also contain grapes from WA, which may be the reason for its incorrect assignment. Healdsburg is in the Sonoma County sitting at the juncture of three major winegrowing regions: Russian River Valley, Dry Creek Valley and Alexander Valley. This is the only sample from Healdsburg that was analyzed, however, the study includes other wines from Sonoma County. Variables entered/removed in the stepwise method of LDA are shown in Table 6 in order of significance. The first step shows silicon to be the most important variable to discriminate between EU and SA followed by manganese in step 2. It is important to note that δD shows to be more important in discriminating the regions appearing in step 3, whereas $\delta^{18}O$ is used in the last step. This provides a means of selecting the most important elements shown between the specific regions of interest if not all elements can be analyzed.

By randomly assigning 80% of samples to a training and the remainder to a prediction set, cross-calibration was performed. Representative model outputs for training and prediction

sets are listed in Table 8, showing that 99.5% and 95.7% of the original grouped cases were correctly classified, respectively.

Table 5. Classification results by region for CA, WA, EU and SA samples.

		Region	Predicted Group Membership				Total
			CA	EU	SA	WA	
Original	Count	CA	15	0	0	1	16
		EU	0	26	0	0	26
		SA	0	0	12	0	12
		WA	1	1	0	62	64
	%	CA	93.8	0	0	6.3	100
		EU	0	100	0	0	100
		SA	0	0	100	0	100
		WA	1.6	1.6	0	96.9	100

97.5% of original grouped cases correctly classified.

Table 6. Variables entered and removed during stepwise method of LDA for World wines.

Step	Variables Entered/Removed		Min. D Squared		Exact F		Sig.	
	Entered	Removed	Statistic	Between Groups	Statistic	df1		df2
1	Si		0.422	EU and SA	3.467	1	114	0.065
2	Mn		2.687	EU and SA	10.933	2	113	4.57E-05
3	Delta D		4.929	CA and SA	11.069	3	112	2.03E-06
4	Re		9.517	CA and SA	15.885	4	111	2.61E-10
5	TI		13.685	CA and EU	26.157	5	110	2.52E-17
6	U		16.572	CA and WA	33.804	6	109	8.95E-23
7	Zn		18.456	EU and SA	20.509	7	108	2.63E-17
8	Pb		20.438	EU and SA	19.688	8	107	5.86E-18
9	Na		21.276	CA and WA	28.136	9	106	2.63E-24
10	Cs		23.879	EU and SA	18.058	10	105	9.78E-19
11	Rb		24.398	CA and WA	25.901	11	104	5.28E-25
12	Sr		27.047	CA and EU	20.17	12	103	6.47E-22
13		Cs	25.589	CA and WA	27.164	11	104	8.98E-26
14	Ni		28.477	EU and SA	17.604	12	103	6.48E-20
15	Ce		28.855	CA and WA	25.421	13	102	2.86E-26
16	Delta O 18		29.564	CA and WA	23.947	14	101	5.97E-26

At each step, the variable that maximizes the Mahalanobis distance between the two closest groups is entered

- Maximum number of steps is 120.
- Minimum partial F to enter is 3.84.
- Maximum partial F to remove is 2.71.
- F level, tolerance, or VIN insufficient for further computation.

Table 7. Standardized canonical discriminant function coefficients for CA, WA, EU and SA wines.

Variables	Function		
	1	2	3
Si	-0.631	0.278	-0.488
Mn	-0.097	0.016	0.64
Delta D	1.424	0.04	-0.095
Re	0.137	0.345	0.84
TI	-0.539	-0.016	-0.896
U	0.281	-0.135	0.689
Zn	0.302	0.343	-0.199
Pb	0.309	-0.624	0.049
Na	0.262	0.359	0.319
Rb	0.314	0.403	0.573
Sr	0.382	0.451	-0.064
Ni	-0.047	0.483	-0.316
Ce	0.073	-0.399	-0.218
Delta O18	-0.521	-0.127	-0.325

Table 8. Classification ability of the LDA model for CA, WA, EU and SA wines.

Group	CA	EU	SA	WA	Total	% correct
Training Set						
CA	23.75	0	0	0	23.75	100
EU	0	23.75	0	0	23.75	100
SA	0	0	23.75	0	23.75	100
WA	0.4481	0	0	23.3	23.75	98.11
Total	24.2	23.75	23.75	23.3	95	99.53
Prediction Set						
CA	5	0	0	0	5	100
EU	0	4	1	0	5	80
SA	0	0	2	0	2	100
WA	0	0	0	11	11	100
Total	5	4	3	11	23	95.65

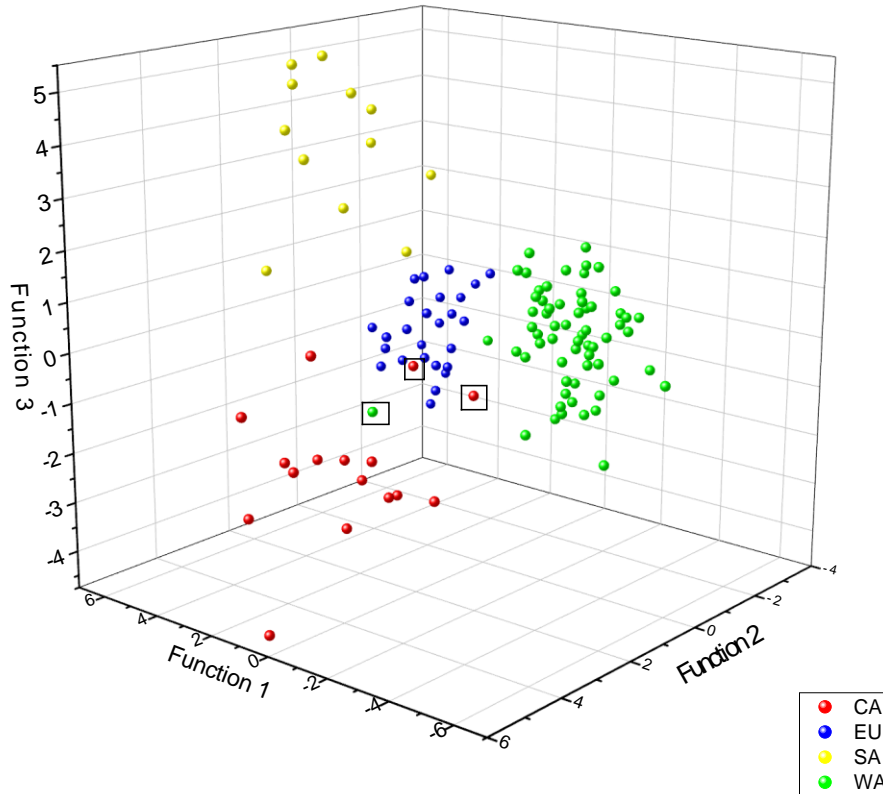


Figure 26. Classification of CA, WA, EU and SA.

When combining WA and CA wines into one North America (NA) region, classification of NA, SA and EU was 99.2% with 1 out of 118 wine samples being incorrectly classified (Table 9). This one sample from NA that was falsely classified as EU is the same one from WA's Columbia Valley (1998 vintage) that had been misclassified as EU. The 14 components from the stepwise method for this LDA are listed in Table 10, showing significant similarities to the previous LDA output. However, in this simpler system with 3 regions, only 2 discriminant functions are used to separate NA, SA and EU wines (Figure 27).

Table 9. Classification results by continent for NA, SA and EU wines.

		Continents	Predicted Group Membership			Total
			EU	NA	SA	
Original	Count	EU	26	0	0	26
		NA	1	79	0	80
		SA	0	0	12	12
	%	EU	100	0	0	100
		NA	1.3	98.8	0	100
		SA	0	0	100	100

99.2% of original grouped cases correctly classified.

Table 10. Standardized canonical discriminant function coefficients for NA, SA and EU wines.

Variables	Function	
	1	2
Delta D	1.793	-0.011
Re	0.18	0.865
Si	-0.809	-0.25
Mn	0.157	0.772
Tl	-0.833	-1.101
U	0.45	0.483
Pb	0.584	-0.278
Rb	0.28	0.934
Delta O 18	-0.561	-0.3
Ce	0.22	-0.364
Ni	-0.453	-0.031
As	0.005	0.563
Na	0.158	0.595
Mo	-0.061	-0.495

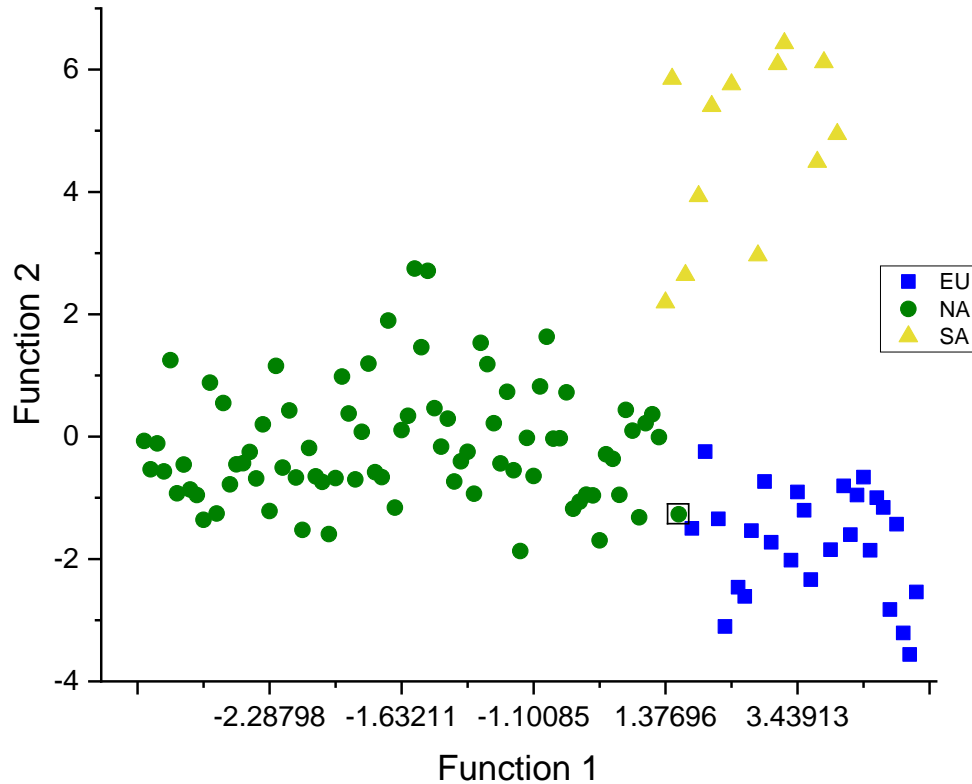


Figure 27. Classification of NA, SA and EU wines.

Placing these results in the context of other published studies, LDA for Argentine wines also showed to achieve a high percentage for the classification of wines (93.2%) from Mendoza, Rio Negro, San Juan and Salta (Azcarate et al., 2015). LDA achieved this with 5 elements: barium, arsenic, lead, molybdenum and cobalt (Azcarate et al., 2015). For the four samples that were not correctly classified in their analysis, authors argued that wine labels may have been incorrect (Azcarate et al., 2015). In a Chinese study of wines from three districts in China, Pengali, Yinchuan and Changli, LDA was also able to distinguish wines satisfactorily (Cheng et al., 2014). LDA was evaluated to discriminate the data by using both “enter independents together” and “use step-wise method” (Cheng et al., 2014). In the first method “enter independents together” eight elements were used to discriminate all three regions with 100%

accuracy (Cheng et al., 2014). In the second, “use step-wise method” only three elements, namely strontium, manganese, and potassium were used to discriminate between the three regions with 100% accuracy (Cheng et al., 2014). The authors determined that “use step-wise method” was optimal for analysis due to the results of the cross-validation methods performed (Cheng et al., 2014).

CONCLUSION

Using advanced analytical instrumentation and statistical tools, concentrations of 60 elements and water stable isotopes were quantified in 118 different wines from 4 regions on 3 continents. Excellent geographical classification was obtained for these wines using LDA and the model was tested showing 99.5% and 95.7% correct classification in the training and prediction sets, respectively. The 14 important classifiers, in order of significance, included silicon, manganese, δD , rhenium, thallium, uranium, zinc, lead, sodium, rubidium, strontium, nickel, cerium and $\delta^{18}O$. PCA provided insight into the various sources of elements; while most were soil-derived, contributing significantly to regional classification, also known as “terroir”, anthropogenic components, such as lead, also played roles in differentiating wines by regions. Water isotopes behaved as anticipated, with lighter isotopes more prevalent in colder climates (WA) and with evapotranspirative losses manifesting in smaller slopes compared to the GMWL, 4-5 vs. 8, respectively. Of particular note was the significantly smaller slope of 2-3 observed in European wines. As European wines are not typically irrigated, this difference in slope may be related to the vines using soil pore waters which tend to display shallower slopes. Results have provided concentrations of 58 elements and 2 water isotopes in wines from all main wine

producing regions in the world, and tools have been developed that successfully classify wines into their regions. To the best of our knowledge, this is the first study of this kind, to try and “fingerprint” WA wines and to set them apart chemically from those produced in other parts of the world.

ACKNOWLEDGEMENTS

This research was partially supported by the School of Graduate Studies and Research, Central Washington University, Ellensburg, Washington. Special thanks are extended to Cox Canyon Vineyard, Wahluke Wine Company, Ginkgo Forest Winery and Yakima Valley Vintners for donating their wines for this study.

REFERENCES

Agilent Technologies. Emmett Soffey. **2017**.

Azcarate, S. M.; Martinez, L. D.; Savio, M.; Camiña, J. M.; Gil, R. A. Classification of Monovarietal Argentinean White Wines by Their Elemental Profile. *Food Control*. **2015**, *57* (May), 268–274 DOI: 10.1016/j.foodcont.2015.04.025.

Cai Community Attributes Inc. Economic & Fiscal Impacts of Wine & Wine Grapes in Washington State. *Washington State Wine*. **2015**.

Cheng, J.; Zhai, Y.; Taylor, D. K. Several Mineral Elements Discriminate the Origin of Wines from Three Districts in China. *Int. J. Food Prop.* **2015**, *18* (7), 1460–1470 DOI: 10.1080/10942912.2014.903415.

Coetzee, P. P.; Van Jaarsveld, F. P.; Vanhaecke, F. Intraregional Classification of Wine via ICP-MS Elemental Fingerprinting. *Food Chem.* **2014**, *164*, 485–492 DOI: 10.

Dinca, O. R.; Ionete, R. E.; Costinel, D.; Geana, I. E.; Popescu, R.; Stefanescu, I.; Radu, G. L. Regional and Vintage Discrimination of Romanian Wines Based on Elemental and Isotopic Fingerprinting. *Food Anal. Methods* **2016**, *9* (8), 2406–2417 DOI: 10.1007/s12161-016-0404-y.

Dunbar, J.; Wilson, A. T. Oxygen and Hydrogen Isotopes in Fruit and Vegetable Juices. *Plant Physiol.* **1983**, 725–727.

Dutra, S. V.; Adami, L.; Marcon, A. R.; Carnieli, G. J.; Roani, C. A.; Spinelli, F. R.; Leonardelli, S.; Ducatti, C.; Moreira, M. Z.; Vanderlinde, R. Determination of the Geographical Origin of Brazilian Wines by Isotope and Mineral Analysis. *Anal. Bioanal. Chem.* **2011**, *401* (5), 1575–1580 DOI: 10.1007/s00216-011-5181-2.1016/j.foodchem.2014.05.027.

Germund, T.; Olsson, T. Plant Uptake of Major and Minor Mineral Elements as Influenced by Soil Acidity and Liming. *Plant Soil.* **2001**, *230*, 307–321.

Gibson, J. J.; Birks, S. J.; Edwards, T. W. D. Global Prediction of δA and $\delta 2H$ - $\delta 18O$ Evaporation Slopes for Lakes and Soil Water Accounting for Seasonality. *Global Biogeochem. Cycles.* **2008**, *22* (2), 1–12 DOI: 10.1029/2007GB002997.

Ingraham, N. L.; Caldwell, E. A. Influence of Weather on the Stable Isotopic Ratios of Wines: Tools for Weather/climate Reconstruction? *J. Geophys. Res.* **1999**, *104* (D2), 2185–2194 DOI: Doi 10.1029/98jd00421.

Mumma, A.; Pinkart, H.; Johansen, A. Final Report for FIPSE Grant on "The Faults of WA Cabernet Sauvignon Wines". **2010**.

Keith, S. K.; Faroon, O.; Roney, N. R.; Scinicariello, F.; Wilbur, S.; Ingerman, L.; Lladós, F.; Plewak, D.; Wohlers, D.; Diamond, G. Toxicological Profile for Uranium. *Toxicol. profiles* **2013**, No. February, 1–526 DOI: <http://dx.doi.org/10.1155/2013/286524>.

Raco, B.; Dotsika, E.; Poutoukis, D.; Battaglini, R.; Chantzi, P. O-H-C Isotope Ratio Determination in Wine in Order to be Used as a Fingerprint of Its Regional Origin. *Food Chem.* **2015**, *168*, 588–594 DOI: 10.1016/j.foodchem.2014.07.043.

Taylor, V. F.; Longerich, H. P.; Greenough, J. D. Multielement Analysis of Canadian Wines by Inductively Coupled Plasma Mass Spectrometry (ICP-MS) and Multivariate Statistics. *J. Agric. Food Chem.* **2003**, *51* (4), 856–860 DOI: 10.1021/jf025761v.

SUPPLEMENTARY INFORMATION

Table 11. ANOVA results for wines from CA, WA, SA and EU. Significances ≤ 0.05 are marked in green.

Element	Region	N	Mean(ppb)	Std. Deviation	Sig.
B	CA	16	7.28E+03	1.41E+03	
	WA	64	5.87E+03	2.29E+03	
	SA	12	7.81E+03	2.05E+03	
	EU	26	5.90E+03	1.31E+03	
	Total	118	6.27E+03	2.08E+03	0.003
Na	CA	16	1.99E+04	1.08E+04	
	WA	64	1.68E+04	1.28E+04	
	SA	12	2.82E+04	7.52E+03	
	EU	26	1.32E+04	6.32E+03	
	Total	118	1.76E+04	1.15E+04	0.001
Mg	CA	16	2.16E+05	2.16E+05	
	WA	64	1.32E+05	1.17E+05	
	SA	12	9.17E+04	1.17E+04	
	EU	26	9.65E+04	3.97E+04	
	Total	118	1.31E+05	1.23E+05	0.011
Al	CA	16	4.48E+02	1.58E+02	
	WA	64	3.77E+02	1.96E+02	
	SA	12	3.97E+02	8.96E+01	
	EU	26	5.30E+02	2.44E+02	
	Total	118	4.23E+02	2.03E+02	0.011
Si	CA	16	2.36E+04	5.98E+03	
	WA	64	1.78E+04	5.58E+03	

Table 11 (Continued)

Element	Region	N	Mean(ppb)	Std. Deviation	Sig.
P	EU	26	9.59E+03	3.57E+03	
	Total	118	1.63E+04	6.66E+03	0
	CA	16	1.86E+05	3.79E+04	
	WA	64	1.52E+05	4.42E+04	
	SA	12	1.34E+05	3.87E+04	
S	EU	26	1.11E+05	2.66E+04	
	Total	118	1.46E+05	4.54E+04	0
	CA	16	1.50E+05	2.11E+04	
	WA	64	1.18E+05	4.59E+04	
	SA	12	1.57E+05	2.53E+04	
K	EU	26	1.34E+05	3.66E+04	
	Total	118	1.30E+05	4.18E+04	0.002
	CA	16	2.11E+06	2.06E+06	
	WA	64	1.48E+06	1.28E+06	
	SA	12	1.26E+06	2.34E+05	
Ca	EU	26	1.09E+06	1.79E+05	
	Total	118	1.46E+06	1.24E+06	0.067
	CA	16	1.06E+05	7.57E+04	
	WA	64	7.79E+04	7.09E+04	
	SA	12	6.95E+04	8.53E+03	
Ti	EU	26	6.76E+04	1.58E+04	
	Total	118	7.87E+04	6.03E+04	0.209
	CA	16	6.63E+01	3.89E+01	
	EU	26	5.11E+01	3.87E+01	
	SA	12	4.93E+01	3.20E+01	
Mn	WA	64	4.55E+01	5.23E+01	
	Total	118	4.99E+01	4.61E+01	0.458
	CA	16	1.73E+03	7.39E+02	
	WA	64	7.34E+02	1.97E+02	
	SA	12	1.57E+03	8.45E+02	
Fe	EU	26	8.91E+02	2.23E+02	
	Total	118	9.89E+02	5.63E+02	0
	CA	16	1.70E+03	7.53E+02	
	WA	64	1.11E+03	7.36E+02	
	SA	12	2.07E+03	6.92E+02	
Co	EU	26	2.30E+03	1.05E+03	
	Total	118	1.55E+03	9.53E+02	0
	CA	16	4.71E+00	1.37E+00	
	WA	64	2.81E+00	1.08E+00	
	SA	12	3.48E+00	2.11E+00	
	EU	26	2.72E+00	8.90E-01	

Table 11 (Continued)

Element	Region	N	Mean(ppb)	Std. Deviation	Sig.
Ni	Total	118	3.11E+00	1.38E+00	0
	CA	16	3.39E+01	1.12E+01	
	WA	64	1.47E+01	7.60E+00	
	SA	12	1.49E+01	5.23E+00	
	EU	26	1.79E+01	6.11E+00	
Cu	Total	118	1.80E+01	9.94E+00	0
	CA	16	1.60E+02	2.00E+02	
	WA	64	9.70E+01	9.24E+01	
	SA	12	1.15E+02	9.35E+01	
	EU	26	1.44E+02	1.26E+02	
Zn	Total	118	1.18E+02	1.21E+02	0.167
	CA	16	7.70E+02	3.81E+02	
	WA	64	4.11E+02	2.03E+02	
	SA	12	5.33E+02	1.96E+02	
	EU	26	6.18E+02	3.12E+02	
As	Total	118	5.18E+02	2.87E+02	0
	CA	16	2.24E+00	1.71E+00	
	WA	64	2.44E+00	1.65E+00	
	SA	12	3.95E+00	2.01E+00	
	EU	26	1.68E+00	1.23E+00	
Rb	Total	118	2.40E+00	1.71E+00	0.002
	CA	16	2.41E+03	8.09E+02	
	WA	64	7.36E+02	3.26E+02	
	SA	12	2.19E+03	1.60E+03	
	EU	26	1.29E+03	5.05E+02	
Sr	Total	118	1.23E+03	9.25E+02	0
	CA	16	1.21E+03	4.00E+02	
	WA	64	6.96E+02	1.92E+02	
	SA	12	1.12E+03	2.38E+02	
	EU	26	8.04E+02	5.35E+02	
Y	Total	118	8.33E+02	3.82E+02	0
	CA	16	4.43E-01	2.12E-01	
	WA	64	5.40E-01	7.44E-01	
	SA	12	3.40E-01	1.33E-01	
	EU	26	6.44E-01	4.98E-01	
Zr	Total	118	5.29E-01	6.05E-01	0.489
	CA	16	2.18E+01	1.84E+01	
	WA	64	1.70E+01	1.73E+01	
	SA	12	1.61E+01	1.40E+01	
	EU	26	2.34E+01	1.89E+01	
	Total	118	1.90E+01	1.76E+01	0.367

Table 11 (Continued)

Element	Region	N	Mean(ppb)	Std. Deviation	Sig.
Cs	CA	16	1.15E+01	9.60E+00	
	WA	64	1.83E+00	1.72E+00	
	SA	12	4.23E+00	4.03E+00	
	EU	26	4.09E+00	2.22E+00	
	Total	118	3.88E+00	5.12E+00	0
Ba	CA	16	4.65E+02	1.51E+02	
	WA	64	2.87E+02	1.19E+02	
	SA	12	2.43E+02	1.12E+02	
	EU	26	2.31E+02	8.73E+01	
	Total	118	2.94E+02	1.36E+02	0
La	CA	16	3.28E+00	5.15E+00	
	WA	64	4.72E+00	6.25E+00	
	SA	12	1.89E+00	4.23E+00	
	EU	26	5.19E+00	6.35E+00	
	Total	118	4.34E+00	5.98E+00	0.35
Ce	CA	16	2.62E-01	1.79E-01	
	WA	64	3.34E-01	5.05E-01	
	SA	12	3.02E-01	1.22E-01	
	EU	26	1.21E+00	1.60E+00	
	Total	118	5.14E-01	9.09E-01	0
Pr	CA	16	3.67E-02	2.36E-02	
	WA	64	4.98E-02	7.93E-02	
	SA	12	4.18E-02	1.97E-02	
	EU	26	1.40E-01	1.76E-01	
	Total	118	6.71E-02	1.08E-01	0.001
Nd	CA	16	1.71E-01	1.05E-01	
	WA	64	2.16E-01	3.22E-01	
	SA	12	1.82E-01	8.31E-02	
	EU	26	5.57E-01	6.77E-01	
	Total	118	2.81E-01	4.22E-01	0.002
Sm	CA	16	3.67E-02	2.46E-02	
	WA	64	4.99E-02	7.76E-02	
	SA	12	4.26E-02	2.15E-02	
	EU	26	1.09E-01	1.25E-01	
	Total	118	6.03E-02	8.59E-02	0.011
Eu	CA	16	2.79E-02	1.11E-02	
	WA	64	3.17E-02	4.08E-02	
	SA	12	2.41E-02	6.64E-03	
	EU	26	4.53E-02	3.74E-02	
	Total	118	3.34E-02	3.55E-02	0.235
Gd	CA	16	4.03E-02	2.00E-02	

Table 11 (Continued)

Element	Region	N	Mean(ppb)	Std. Deviation	Sig.
Dy	WA	64	6.83E-02	9.86E-02	0.052
	SA	12	3.61E-02	2.19E-02	
	EU	26	1.09E-01	1.17E-01	
	Total	118	7.02E-02	9.41E-02	
	CA	16	4.61E-02	1.85E-02	
Ho	WA	64	6.09E-02	8.51E-02	0.117
	SA	12	3.51E-02	1.89E-02	
	EU	26	9.74E-02	1.24E-01	
	Total	118	6.43E-02	8.74E-02	
	CA	16	1.24E-02	5.14E-03	
Er	WA	64	1.52E-02	1.78E-02	0.258
	SA	12	8.81E-03	4.03E-03	
	EU	26	1.90E-02	1.65E-02	
	Total	118	1.50E-02	1.56E-02	
	CA	16	4.56E-02	1.93E-02	
Tm	WA	64	5.33E-02	5.33E-02	0.347
	SA	12	3.80E-02	2.12E-02	
	EU	26	6.44E-02	4.38E-02	
	Total	118	5.32E-02	4.57E-02	
	CA	16	8.70E-03	4.59E-03	
Yb	WA	64	9.49E-03	7.36E-03	0.38
	SA	12	5.94E-03	2.85E-03	
	EU	26	8.92E-03	5.99E-03	
	Total	118	8.90E-03	6.43E-03	
	CA	16	6.29E-02	3.01E-02	
Re	WA	64	6.59E-02	5.41E-02	0.572
	SA	12	4.53E-02	2.87E-02	
	EU	26	6.68E-02	4.72E-02	
	Total	118	6.36E-02	4.78E-02	
	CA	16	4.02E-02	6.48E-02	
Hg	WA	64	5.00E-02	3.96E-02	0
	SA	12	1.17E-01	8.32E-02	
	EU	26	2.38E-02	2.33E-02	
	Total	118	4.97E-02	5.26E-02	
	CA	16	5.44E-01	1.86E+00	
Pb	WA	64	1.03E-01	8.82E-02	0.032
	SA	12	4.58E+00	1.52E+01	
	EU	26	2.19E-01	4.81E-01	
	Total	118	6.43E-01	4.91E+00	
	CA	16	4.65E+00	2.07E+00	
	WA	64	5.18E+00	5.12E+00	

Table 11 (Continued)

Element	Region	N	Mean(ppb)	Std. Deviation	Sig.
Th	SA	12	6.56E+00	4.48E+00	
	EU	26	1.47E+01	7.94E+00	
	Total	118	7.35E+00	6.76E+00	0
	CA	16	1.18E-01	6.86E-02	
	WA	64	2.17E-01	2.49E-01	
	SA	12	1.46E-01	1.43E-01	
U	EU	26	1.60E-01	1.11E-01	
	Total	118	1.84E-01	2.00E-01	0.231
	CA	16	5.38E-01	6.91E-01	
	WA	64	6.59E-01	9.56E-01	
	SA	12	5.52E-01	4.40E-01	
	EU	26	3.61E-01	2.50E-01	
Delta O-18	Total	118	5.66E-01	7.74E-01	0.433
	CA	16	8.04E+00	4.38E+00	
	WA	64	1.08E+00	2.22E+00	
	SA	12	3.92E+00	1.89E+00	
	EU	26	5.27E+00	3.31E+00	
	Total	118	3.24E+00	3.80E+00	0
Delta D	CA	16	9.37E+00	2.31E+01	
	WA	64	-4.24E+01	1.35E+01	
	SA	12	-3.73E+00	1.14E+01	
	EU	26	1.17E+01	8.88E+00	
	Total	118	-1.95E+01	2.89E+01	0

Table 12. PCA factor loadings for wines from CA, WA, SA and EU. Loadings with values ≥ 0.5 are marked in green.

Variables	Principal Components							
	PC 1	PC 2	PC 3	PC 4	PC 5	PC 6	PC 7	PC 8
% Variance	17.45	9.79	5.51	5.2	5.14	4.99	4.17	4.12
Li	-0.093	0.021	0.234	-0.249	0.106	0.721	-0.365	0.076
Be	0.144	0.025	-0.027	-0.006	0.254	0.063	0.012	-0.05
B	-0.173	0.117	0.197	0.2	0.144	0.17	-0.121	-0.035
Na	0.127	0.086	0.142	-0.075	0.068	-0.248	0.092	-0.037
Mg	-0.096	0.096	-0.043	0.942	-0.022	-0.119	0.014	-0.053
Al	0.504	0.121	0.042	-0.015	0.428	-0.045	0.012	-0.039
Si	-0.046	0.256	-0.089	0.188	0.075	-0.228	0.698	-0.071
P	-0.342	0.318	-0.044	0.299	0.017	-0.092	-0.062	0.048
S	0.125	0.438	0.175	0.074	-0.074	-0.507	0.105	0.093
K	-0.133	0.06	0.002	0.902	-0.03	-0.155	-0.007	-0.025
Ca	0.037	0.027	-0.025	0.86	0.045	-0.072	0.039	-0.093

Table 12 (Continued)

Variables	PC 1	PC 2	PC 3	PC 4	PC 5	PC 6	PC 7	PC 8
% Variance	17.45	9.79	5.51	5.2	5.14	4.99	4.17	4.12
Ti	0.08	0.13	0.049	0.2	-0.023	-0.057	0.036	-0.058
V	0.393	0.136	-0.094	0.04	0.652	-0.011	-0.13	0.029
Mn	-0.038	0.815	0.006	-0.029	0.156	-0.038	0.114	-0.028
Fe	0.075	0.259	-0.035	-0.189	0.387	-0.135	-0.152	0.085
Co	0.059	0.708	-0.062	0.03	0.224	0.166	0.113	-0.012
Ni	0.084	0.736	-0.067	0.266	-0.059	0.04	0.23	-0.054
Cu	-0.098	0.107	-0.133	-0.097	-0.08	0.184	-0.083	-0.048
Zn	-0.015	0.44	-0.079	0.055	0.267	0.035	-0.207	-0.12
Ga	0.746	0.192	0.025	0.045	0.44	-0.049	0.06	0.034
As	0.129	-0.072	0.28	0.054	0.583	0.116	-0.136	-0.087
Se	0.129	0.264	0.129	0.11	-0.149	0.114	-0.051	0.063
Rb	-0.02	0.853	-0.031	-0.024	0.111	-0.092	-0.205	0.082
Sr	0.095	0.339	0.071	-0.048	0.335	-0.006	0.216	-0.198
Y	0.486	-0.026	-0.034	-0.015	0.08	0.047	0.093	-0.017
Zr	0.109	0.21	0.043	-0.144	0.023	0.722	0.026	0.272
Mo	0.186	-0.014	-0.086	-0.009	0.447	0.098	0.006	0.202
Pd	-0.037	-0.057	0.777	-0.074	0.017	-0.113	-0.035	-0.001
Ag	0.094	-0.025	-0.003	0.253	0.044	-0.294	0.495	-0.184
Cd	0.044	0.325	-0.096	0.148	0.082	-0.157	0.27	0.044
Sn	-0.001	-0.183	-0.004	0.01	-0.098	0.04	0.059	0.076
Sb	0.07	0.221	0.005	-0.029	0.789	0.113	0.075	-0.015
Cs	0.078	0.769	-0.034	-0.001	0.016	-0.097	-0.179	0.027
Ba	-0.146	0.461	-0.025	0.026	-0.05	0.226	0.223	0.051
La	0.054	-0.048	0.095	-0.105	0.015	0.874	-0.105	0.102
Ce	0.913	-0.011	0.002	-0.025	0.097	-0.019	-0.165	-0.019
Pr	0.921	-0.01	-0.016	-0.044	0.085	0.03	-0.173	-0.016
Nd	0.943	0.003	-0.011	-0.041	0.088	0.052	-0.143	-0.011
Sm	0.971	0.022	-0.001	-0.032	0.084	-0.007	-0.011	0.003
Eu	0.49	-0.007	-0.001	-0.084	0.1	0.122	-0.092	-0.004
Gd	0.955	-0.016	0.014	-0.029	0.008	-0.045	0.162	0.01
Dy	0.959	-0.003	0.005	-0.015	0.012	-0.048	0.118	-0.011
Ho	0.934	0.032	0.017	-0.016	-0.015	0.038	0.169	0.002
Er	0.832	0.034	0.04	-0.048	-0.002	-0.089	0.157	0.014
Tm	0.809	0.081	0.054	-0.013	0.011	0.04	0.229	0.03
Yb	0.767	0.139	0.047	-0.02	0.089	0.203	0.192	0.035
Hf	-0.038	-0.039	0.068	-0.093	-0.055	0.119	-0.064	0.901
Ta	0.061	-0.083	0.837	-0.031	-0.055	0.088	0.199	0.285
W	0.18	0.066	0.073	-0.004	0.645	-0.074	0.052	0.604
Re	-0.1	-0.103	0.065	-0.139	0.075	-0.031	-0.017	-0.062
Ir	0.128	-0.031	0.881	0.024	0.039	0.192	-0.063	0.145

Table 12 (Continued)

Variables	PC 1	PC 2	PC 3	PC 4	PC 5	PC 6	PC 7	PC 8
% Variance	17.45	9.79	5.51	5.2	5.14	4.99	4.17	4.12
Pt	0.012	-0.095	0.275	-0.183	0.035	0.41	-0.13	0.331
Au	-0.022	0.074	0.094	-0.071	0.066	0.177	-0.02	0.859
Hg	-0.037	0.016	0.865	0.004	0.049	0.064	-0.017	-0.146
Tl	0.182	0.783	-0.017	0.036	0.059	0.058	0.108	0.036
Pb	0.205	-0.026	0.025	-0.037	0.025	-0.035	0.008	-0.054
Th	0.305	-0.138	0.056	-0.181	-0.046	-0.095	0.654	-0.024
U	0.472	0.065	0.182	0.067	-0.073	-0.179	0.571	0.056
Delta O-18	-0.093	0.622	-0.024	0.11	-0.138	0.048	0.042	0
Delta D	0.04	0.6	-0.005	0.007	-0.067	0.029	-0.152	-0.023

CHAPTER IV

WASHINGTON STATE WINES

Multielement Analysis

To investigate the potential for WA wine classification to their regions, 60 samples from WA were subjected to the same ANOVA, PCA and LDA including 39 elements and $\delta^{18}\text{O}$ and δD . These regions are labeled WA1 through WA7. Examination of the combined statistical outputs resulted in the selection of 7 most descriptive components that also displayed high inter-regional variabilities. The concentrations of these elements are summarized in box-and-whisker plots in Figures 28 and 29, arranged in order of decreasing concentrations, and the additional components $\delta^{18}\text{O}$ and δD are presented in the following section. Analogous to the World Wines (WW) plots, for better visualization, outliers were omitted and elements arranged by concentrations.

Results and discussion for WA wines are accompanied with comparisons between the PCA outcomes with WW as significant similarities and differences could be found. For instance, PC1, PC2 and PC5 from the WA PCA seemed to appear combined in PC1 for the WW. Specifically, the lanthanides, which are divided into light and heavy rare earth elements (LREE and HREE) all appeared in PC1 for WW, while for WA some of the LREE appeared in PC5 (5.9% variance) and all the HREE and a few LREE in PC1 (20.0% variance). Representative elements for LREE in PC5 and HREE in PC1 are shown in Figure 29 for praseodymium and gadolinium, respectively. Gadolinium is also one of the components used in LDA. WA2 wines have the highest gadolinium concentrations showing significant inter-regional variability as indicated by

the Tukey's test p-values. Praseodymium in PC5, shows significant differences for 5 comparison pairs between WA2 and other regions.

Aluminum, a soil derived element, was in PC1 for WW, however, for WA wines it showed up separately in PC2 (8.0% variance). Aluminum does not show significant differences between regions or proved to be important in LDA. Another set of PCs that carry close resemblance between the WW and WA wines are WW PC2 and WA PC3 (6.8% variance), both contain manganese, rubidium and the water isotopes, all of which are soil/water derived. Both aluminum and manganese are shown in Figure 28C. Manganese is not significantly different between regions nor proved to be important in LDA for WA wines, while it was the second most important in LDA for the WW, with rubidium and the water isotopes also being very important differentiators. Silicon is plotted in Figure 28B and shows significantly higher concentrations in WA2 wines; however, it does not emanate as important in the LDA as a classifying element. In contrast, in the WW LDA, silicone was the most important of all components to differentiate wines, in particular between EU and SA (see Table 7). Barium, also a soil derived element, appears on its own in PC11 (variance 3.6%) and is significant in LDA for the separation of WA wines into their regions, appearing in fourth place. Previous studies have demonstrated barium to be useful for geographical classification. For instance, in an Argentine study, wines from Salta were clearly separated by their higher barium concentrations (Azcarate et al., 2015), and in a South African study, red wines averaging 105, 200 and 338 ppb barium for 3 different regions, found barium as a discriminant element for two of the regions (Coetzee et al., 2014). In our study, WA6 wines have the highest average barium concentrations of 465 ppb, the difference is statistically significant compared to WA1, WA2, WA3 and WA5.

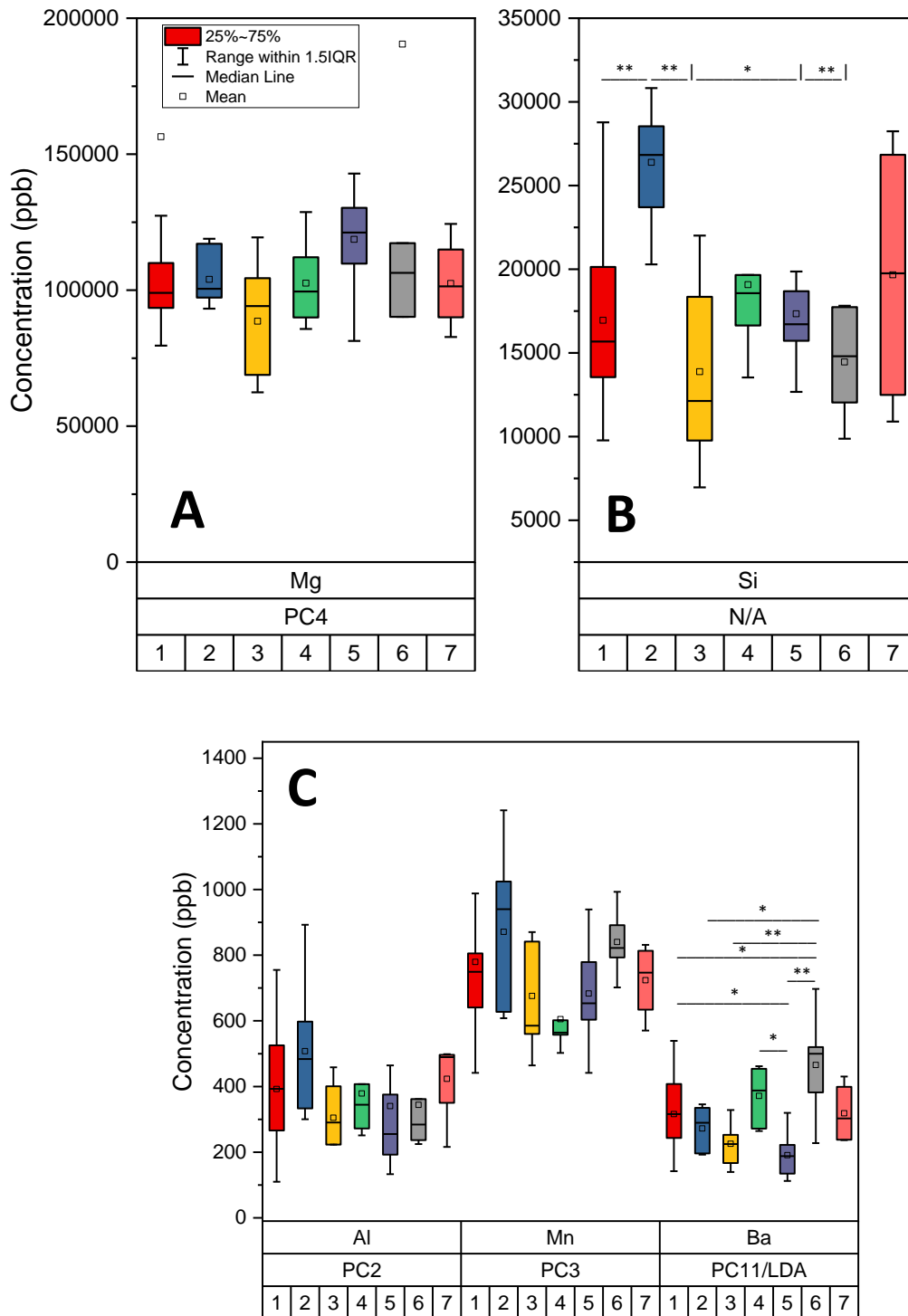


Figure 28. Box-and-whisker plots of selected elements in WA wines, grouped by regions WA1 through WA7: **A.** Magnesium, **B.** Silicon and **C.** Aluminum, manganese and barium.

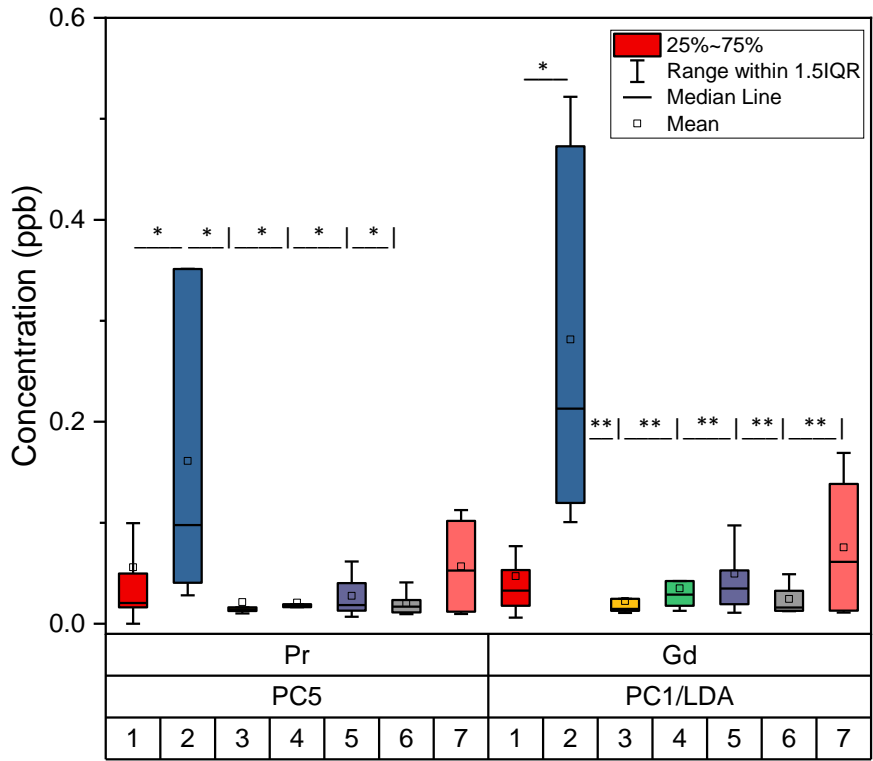


Figure 29. Box-and-whisker plots of selected elements in WA wines, grouped by regions WA1 through WA7: Praseodymium and gadolinium

Major cations, including magnesium (Figure 28A), potassium and calcium appear in PC4 (6.4% variance), identical to where they appeared in WW PCA. None of these elements show inter-regional variability nor were they used in the LDA.

Metals from mining and smelting, including mercury which was found significant in SA wines, does not appear in the WA PCA. The anthropogenic elements arsenic and lead appear in the less significant PCs, PC14 and PC13, respectively.

Isotope Analysis

For WA water isotopes, both $\delta^{18}\text{O}$ or δD showed significance between the same pair of regions as seen by Figures 30 and 31. They also appear in the same PC3 which accounts for 6.8% of the variance, correlating with the rubidium/manganese soil component. Neither $\delta^{18}\text{O}$ or δD were extracted in LDA, however. Note that only 1 comparison pair for $\delta^{18}\text{O}$ or δD is

significantly different in this dataset: between WA1 and WA5. WA1 wines have higher $\delta^{18}\text{O}$ and δD ratios in comparison to WA5. While both regions are arid, WA5 is one of the warmest and driest regions allowing for nearly complete control of grape ripening and vine vigor through irrigation, which would imply that the water isotopic signature is closely related to the irrigation water that has been subjected to LEL which leaves behind heavier water. This is not what we observe. WA1, located in an arid and semi-arid climate, receives 6-8 inches of precipitation annually, which is supplemented by irrigation. This precipitated water would have a lighter signature compared to the irrigation water thus leading to an overall lighter water in WA1 wines. Again, this is opposite of what we observe. It seems that other factors are controlling the water isotopic composition in these wine samples.

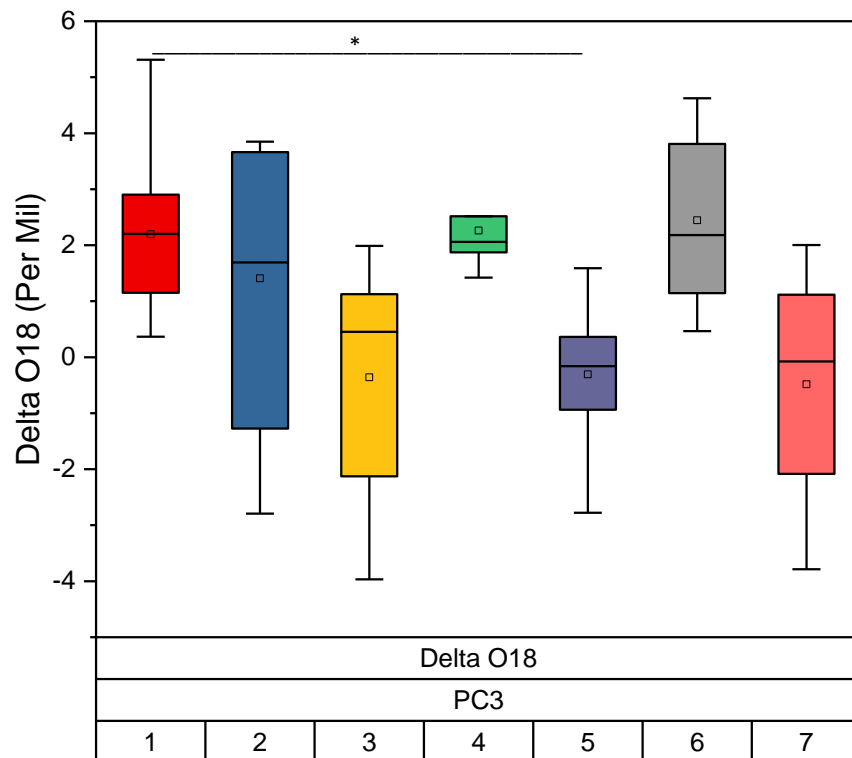


Figure 30. Box-and-whisker plot of $\delta^{18}\text{O}$ in WA wines, grouped by regions WA1 through WA7.

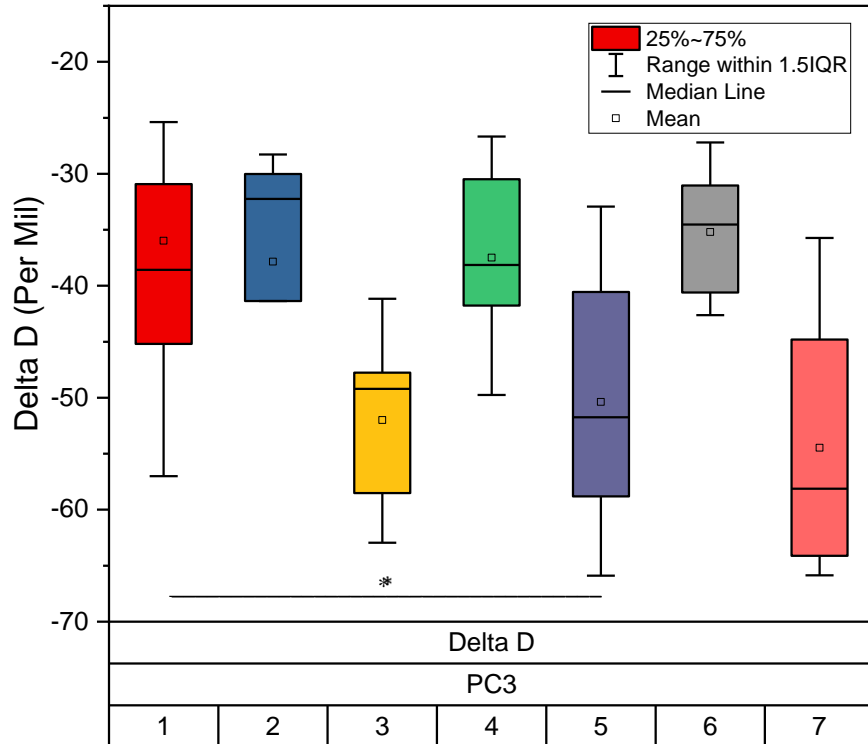


Figure 31. Box-and-whisker plot of δD in WA wines, grouped by regions WA1 through WA7.

Water isotopes are plotted together in Figure 32, ranging from -4.97 to 5.31 ‰ for $\delta^{18}O$ values and -65.89 to -26.67 ‰ for δD values. Aside from including the GMWL, the meteoric water lines of Hanford and Ellensburg are plotted as well (USGS). The isotopic composition for the two general regions is similar. In comparing slopes of least-squares-fit lines for each region, WA4 (N=6, $R^2=0.592$) wines have the highest slope of 8.5, which is higher than the GMWL slope of 8, while WA3 (N=7, $R^2=0.570$) and WA6 (N=5, $R^2=0.374$) wines' slopes are 2.6 and 2.3, respectively. The remainder of the samples (N=42) have slopes of 4.1 and 4.8 in their respective regions, which are expected values. As explained in the WW section, lines falling below the MWLs are indicative of evapo(transpi)rative losses. Shallower lines, i.e., lower slopes, may indicate the lack of irrigation with surface waters, as seen for EU wines. Based on this explanation, WA3 and WA6 should be located in regions where irrigation is less common,

thus in higher precipitation regions. However, this is not the case. With R^2 values between 0.37 and 0.60, properly interpreting these differences in slopes between regions is not straightforward.

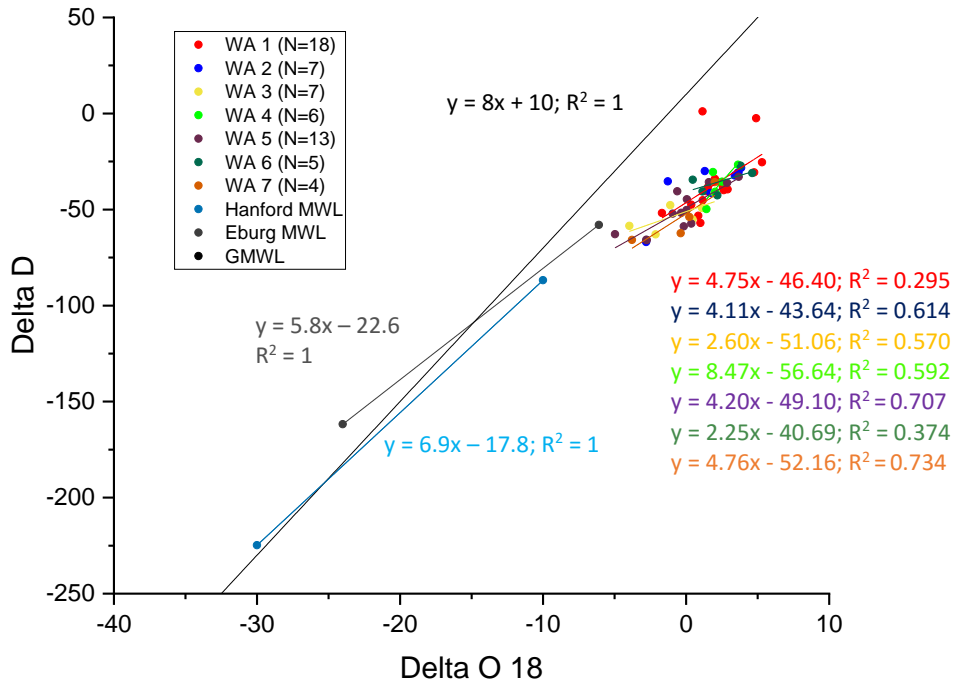


Figure 32. Plot of delta deuterium versus $\delta^{18}\text{O}$ for WA wines.

Geographical Discrimination Analysis

Seven different regions were assigned to the 60 WA wines for classification with LDA: 6 from the different American Viticulture Areas (AVA) and 1 from a vineyard (WA2) that although is far removed from the rest, is currently classified as WA1. LDA used different variables in comparison to the LDA components from the WW (Table 7). Overall, classification was significantly less compared to the WW LDA outcome. Wines from the various regions were falsely assigned, mostly classified as WA1, which is the region with the most wines (N=18). This close relationship of many wines with WA1 is not unexpected, as all other growing regions are

considered sub-appellations of WA1. WA1 is located in central, south-central and south-eastern WA representing a third of the state's land mass, making it difficult to differentiate between the smaller AVAs within and adjacent to its borders. Regions that have a higher percentage of classification are more clearly seen to be discriminated. These regions include WA2, WA3 and WA5, with WA5 having the highest classification. WA5 sits on a large alluvial fan giving a deep wind-blown sand type of soil. WA3 has three soil types in the area: wind-blown sand and loess, Missoula flood sediment and hill slope rubble from the Columbia river basalt bedrock. All three soil types provide for well-drained soils appropriate for vines. This AVA is also close to the Columbia River which creates 30% more wind, toughening grape skins and causes moderating effect on temperatures.

CHAPTER V

CONCLUSION

The presented research has highlighted in detail the elemental and water isotopic compositions of various wines around the world with the goal of geographically discriminating wines between regions, including California (CA) and Washington (WA), in the USA, South America (SA) and Europe (EU). Using linear discriminant analysis (LDA) on the 118 distinct wine samples, a high degree of classification (97.5%) was obtained for the 4 mentioned regions. Fourteen classifiers were extracted in the forward step-wise approach. In order of significance these components consisted of silicon, manganese, delta deuterium, rhenium, thallium, uranium, zinc, lead, sodium, rubidium, strontium, nickel, cerium and $\delta^{18}\text{O}$. Rubidium has been seen as a strong classifier in other studies. PCA and ANOVA outputs contributed to interpretation of elemental sources, revealing that most elements of significance were soil-derived, including rubidium, and that smaller, anthropogenic components, characterized by lead and a few other heavy elements, also played roles in discriminating wines. Water isotope data showed that wine samples from WA had concentrations in the lighter range, as expected in colder climates, whereas CA, SA and EU wines were heavier. Due to the expected fractionation of water isotopes from evapotranspiration, all wine samples lay below the GMWL. This is consistent with other published works. Combining WA and CA wines into one region, increased classification of NA, SA and UE to 99.2% with one out of 118 wine samples incorrectly classified.

The model for WA wines resulted in low classification of samples to their respective regions. These observations are not unanticipated as 6 of the 7 regions are considered sub-

appellations of the one.

To the best of our knowledge, this is the first study to “fingerprint” WA wines. A data base has been initiated that contains elemental and water isotopic concentrations of wines from 4 major wine producing regions of the world. The combination of certain elemental and isotopic composition, and statistical analysis, has proven to be an effective tool to assign wines to their geographical origin. This tool has the potential to play a significant role in identifying and preventing wine fraud on WA wines.

REFERENCES

- Abdi, H.; Williams, L. J. Principal Component Analysis. *Wiley Interdiscip. Rev. Comput. Stat.* **2010**, 2 (4), 433–459 DOI: 10.1002/wics.101.
- Agilent Technologies. Agilent 7500 Series ICP-MS Hardware Manual. **2008**.
- Agilent Technologies. Agilent 8900 Triple Quadrupole ICP-MS Hardware Maintenance Manual. **2016**.
- Ambler, P. China Is Facing an Epidemic of Counterfeit and Contraband Wine. *Forbes*, July 27, 2017.
- Azcarate, S. M.; Martinez, L. D.; Savio, M.; Camiña, J. M.; Gil, R. A. Classification of Monovarietal Argentinean White Wines by Their Elemental Profile. *Food Control.* **2015**, 57 (May), 268–274 DOI: 10.1016/j.foodcont.2015.04.025.
- Bolea-Fernandez, E.; Balcaen, L.; Resano, M.; Vanhaecke, F. Overcoming Spectral Overlap via Inductively Coupled Plasma-Tandem Mass Spectrometry (ICP-MS/MS). A Tutorial Review. *J. Anal. At. Spectrom.* **2017** DOI: 10.1039/C7JA00010C.
- Cai Community Attributes Inc. Economic & Fiscal Impacts of Wine & Wine Grapes in Washington State. *Washington State Wine.* **2015**.
- Cheng, J.; Zhai, Y.; Taylor, D. K. Several Mineral Elements Discriminate the Origin of Wines from Three Districts in China. *Int. J. Food Prop.* **2015**, 18 (7), 1460–1470 DOI: 10.1080/10942912.2014.903415.
- Coetzee, P. P.; Steffens, F. E.; Eiselen, R. J.; Augustyn, O. P.; Balcaen, L.; Vanhaecke, F. Multi-Element Analysis of South African Wines by ICP-MS and Their Classification according to Geographical Origin. *J. Agric. Food Chem.* **2005**, 53 (13), 5060–5066 DOI: 10.1021/jf048268n.
- Coetzee, P. P.; Van Jaarsveld, F. P.; Vanhaecke, F. Intraregional Classification of Wine via ICP-MS Elemental Fingerprinting. *Food Chem.* **2014**, 164, 485–492 DOI: 10.
- Collins, T. S. The Impact of Vineyard Origin and Red Wines. *Agilent Technologies.* **2015**.
- Cumming, E. The Great Wine Fraud. *The Guardian*. September 10, 2016.
- Dinca, O. R.; Ionete, R. E.; Costinel, D.; Geana, I. E.; Popescu, R.; Stefanescu, I.; Radu, G. L. Regional and Vintage Discrimination of Romanian Wines Based on Elemental and Isotopic Fingerprinting. *Food Anal. Methods* **2016**, 9 (8), 2406–2417 DOI: 10.1007/s12161-016-0404-y.

- Dunbar, J.; Wilson, A. T. Oxygen and Hydrogen Isotopes in Fruit and Vegetable Juices. *Plant Physiol.* **1983**, 725–727.
- Dutra, S. V.; Adami, L.; Marcon, A. R.; Carnieli, G. J.; Roani, C. A.; Spinelli, F. R.; Leonardelli, S.; Ducatti, C.; Moreira, M. Z.; Vanderlinde, R. Determination of the Geographical Origin of Brazilian Wines by Isotope and Mineral Analysis. *Anal. Bioanal. Chem.* **2011**, 401 (5), 1575–1580 DOI: 10.1007/s00216-011-5181-2.1016/j.foodchem.2014.05.027.
- Falkowski, P. G.; Scholes, R. J.; Boyle, E.; Canadell, J.; Canfield, D.; Elser, J.; Gruber, N.; Hibbard, K.; Högberg, P.; Linder, S.; Mackenzie, F. T.; Moore, B.; Pedersen, T.; Rosenthal, Y.; Seitzinger, S.; Smetacek, V.; Steffen, W. The Global Carbon Cycle: A Test of Our Knowledge of Earth as a System. *Science (80-.)*. **2000**, 290 (5490), 291–296 DOI: 10.1126/science.290.5490.291.
- Fan, S.; Zhong, Q.; Gao, H.; Wang, D.; Li, G.; Huang, Z. Elemental Profile and Oxygen Isotope Ratio ($\delta^{18}\text{O}$) for Verifying the Geographical Origin of Chinese Wines. *J. Food Drug Anal.* **2018**, No. 2017, 1–12 DOI: 10.1016/j.jfda.2017.12.009.
- Germund, T.; Olsson, T. Plant Uptake of Major and Minor Mineral Elements as Influenced by Soil Acidity and Liming. *Plant Soil.* **2001**, 230, 307–321.
- Gibson, J. J.; Birks, S. J.; Edwards, T. W. D. Global Prediction of δA and $\delta^{2}\text{H}$ - $\delta^{18}\text{O}$ Evaporation Slopes for Lakes and Soil Water Accounting for Seasonality. *Global Biogeochem. Cycles.* **2008**, 22 (2), 1–12 DOI: 10.1029/2007GB002997.
- Greenough, J. D.; Longerich, H. P.; Jackson, S. E. Element Fingerprinting of Okanagan Valley Wines Using ICP – MS : Relationships between Wine Composition, Vineyard and Wine Colour. *Aust. J. Grape Wine Res.* **1997**, 3, 75–83 DOI: 10.1111/j.1755-0238.1997.tb00118.x.
- Harde, H. Scrutinizing the Carbon Cycle and CO₂ Residence Time in the Atmosphere. *Glob. Planet. Change* **2017**, 152, 19–26 DOI: 10.1016/j.gloplacha.2017.02.009.
- Hooda, P. S. *Trace Elements in Soil*: John Wiley & Sons Ltd; United Kingdom, **2010**. Vol. 1.
- Iannone, R. Q.; Romanini, D.; Cattani, O.; Meijer, H. A. J.; Kerstel, E. R. T. Water Isotope Ratio ($\delta^{2}\text{H}$ and $\delta^{18}\text{O}$) Measurements in Atmospheric Moisture Using an Optical Feedback Cavity Enhanced Absorption Laser Spectrometer. *J. Geophys. Res.* **2010**, 115 (D10), D10111 DOI: 10.1029/2009JD012895.
- Ingraham, N. L.; Caldwell, E. A. Influence of Weather on the Stable Isotopic Ratios of Wines: Tools for Weather/climate Reconstruction? *J. Geophys. Res.* **1999**, 104 (D2), 2185–2194 DOI: Doi 10.1029/98jd00421.

- International Atomic Energy Agency. GNIP Maps and Animations. **2001**.
- Jakubowski, N.; Brandt, R.; Stuewer, D.; Eschnauer, H. R.; Gortges, S. Analysis of Wines by ICP-MS: Is the Pattern of the Rare Earth Elements a Reliable Fingerprint for the Provenance? *Fresenius. J. Anal. Chem.* **1999**, *364* (5), 424–428 DOI: 10.1007/s002160051361.
- Keith, S. K.; Faroon, O.; Roney, N. R.; Scinicariello, F.; Wilbur, S.; Ingerman, L.; Llados, F.; Plewak, D.; Wohlers, D.; Diamond, G. Toxicological Profile for Uranium. *Toxicol. profiles* **2013**, No. February, 1–526 DOI: <http://dx.doi.org/10.1155/2013/286524>.
- Martin, G. J.; Guillou, C.; Martin, M. L.; Cabanis, M. T.; Tep, Y.; Aerny, J. Natural Factors of Isotope Fractionation and the Characterization of Wines. *J. Agric. Food Chem.* **1988**, *36* (2), 316–322 DOI: 10.1021/jf00080a019.
- Morgan, J. Wines Scientists Find ‘Fingerprints’ of Region and Quality. *BBC News*. **2014**.
- Mumma, A.; Pinkart, H.; Johansen, A. Final Report for FIPSE Grant on "The Faults of WA Cabernet Sauvignon Wines". **2010**.
- Mustacich, S. Massive Rhône Valley Wine Fraud Reported by French Authorities. *Wine Spectator*. **2018**.
- Needham, K. Chinese Police Find 14,000 Bottles of Fake Penfolds Wine in Counterfeiting Scam. *The Sydney Morning Herald*. **2017**.
- Picarro Inc. Cavity Ring-Down Spectroscopy (CRDS). *Picarro*. **2016**.
- Raco, B.; Dotsika, E.; Poutoukis, D.; Battaglini, R.; Chantzi, P. O-H-C Isotope Ratio Determination in Wine in Order to be Used as a Fingerprint of its Regional Origin. *Food Chem.* **2015**, *168*, 588–594 DOI: 10.1016/j.foodchem.2014.07.043.
- Shen, A. Fake Wine in China. *China Policy Institute:Analysis*. **2017**.
- Skoog, D. A.; Holler, F. J.; Crouch, S. R. *Principles of Instrumental Analysis*: Cengage Learning; Australia, **2007, 2018**. Print.
- Sugiyama, N.; Nakano, K. Reaction Data for 70 Elements Using O₂, NH₃ and H₂ Gases with the Agilent 8800 Triple Quadrupole ICP-MS Technical Note. **2014**, 1–14.
- Tan, P.-N.; Steinbach, M.; Kumar, V. Chap 8 : Cluster Analysis: Basic Concepts and Algorithms. *Introd. to Data Min.* **2005**, Chapter 8 DOI: 10.1016/0022-4405(81)90007-8.

Taylor, V. F.; Longerich, H. P.; Greenough, J. D. Multielement Analysis of Canadian Wines by Inductively Coupled Plasma Mass Spectrometry (ICP-MS) and Multivariate Statistics. *J. Agric. Food Chem.* **2003**, *51* (4), 856–860 DOI: 10.1021/jf025761v.

Tissue, B.M. Quadrupole Mass Spectrometry. *The Chemistry Hypermedia Project.* **2000**.

Wolf, R. E. What Is ICP-MS? ... and More Importantly, What Can it Do? *U.S. Geol. Surv. Crustal Geophys. Geochemistry Sci. Cent.* **2005**, *7*.

APPENDICES

Appendix A-ANOVA results for wines from WA regions.

Element	Region	N	Mean(ppb)	Std. Deviation	Sig.
B	WA1	18	6.12E+03	1.89E+03	0
	WA2	7	4.09E+03	1.87E+03	
	WA3	7	6.40E+03	1.40E+03	
	WA4	6	6.20E+03	7.98E+02	
	WA5	13	4.57E+03	1.67E+03	
	WA6	5	1.02E+04	2.98E+03	
	WA7	4	5.64E+03	1.68E+03	
	Total	60	5.89E+03	2.31E+03	
Na	WA1	18	1.53E+04	5.83E+03	0.05
	WA2	7	2.19E+04	1.44E+04	
	WA3	7	3.01E+04	2.98E+04	
	WA4	6	1.77E+04	7.97E+03	
	WA5	13	1.06E+04	4.83E+03	
	WA6	5	1.20E+04	5.22E+03	
	WA7	4	1.68E+04	8.47E+03	
	Total	60	1.68E+04	1.31E+04	
Mg	WA1	18	1.56E+05	1.77E+05	0.639
	WA2	7	1.04E+05	1.01E+04	
	WA3	7	8.86E+04	2.03E+04	
	WA4	6	1.03E+05	1.64E+04	
	WA5	13	1.19E+05	1.66E+04	
	WA6	5	1.90E+05	2.00E+05	
	WA7	4	1.02E+05	1.74E+04	
	Total	60	1.28E+05	1.13E+05	
Al	WA1	18	3.92E+02	1.60E+02	0.588
	WA2	7	5.08E+02	1.99E+02	
	WA3	7	3.05E+02	9.17E+01	
	WA4	6	3.79E+02	1.49E+02	
	WA5	13	3.41E+02	3.11E+02	
	WA6	5	3.44E+02	1.60E+02	
	WA7	4	4.23E+02	1.38E+02	
	Total	60	3.81E+02	1.99E+02	
Si	WA1	18	1.67E+04	4.92E+03	
	WA2	7	2.64E+04	3.49E+03	
	WA3	7	1.39E+04	5.47E+03	
	WA4	6	1.91E+04	4.65E+03	
	WA5	13	1.73E+04	3.77E+03	
	WA6	5	1.45E+04	3.50E+03	

Appendix A (Continued)

Element	Region	N	Mean(ppb)	Std. Deviation	Sig.
P	WA7	4	1.97E+04	8.46E+03	0
	Total	60	1.79E+04	5.73E+03	
	WA1	18	1.67E+05	5.37E+04	
	WA2	7	9.40E+04	2.01E+04	
	WA3	7	1.51E+05	3.55E+04	
	WA4	6	1.57E+05	3.76E+04	
	WA5	13	1.51E+05	2.46E+04	
	WA6	5	1.89E+05	3.72E+04	
S	WA7	4	1.43E+05	5.07E+04	0.005
	Total	60	1.52E+05	4.54E+04	
	WA1	18	1.11E+05	2.76E+04	
	WA2	7	1.55E+05	5.01E+04	
	WA3	7	1.04E+05	4.22E+04	
	WA4	6	1.12E+05	2.72E+04	
	WA5	13	1.32E+05	7.09E+04	
	WA6	5	1.20E+05	1.88E+04	
K	WA7	4	9.49E+04	3.50E+04	0.246
	Total	60	1.20E+05	4.59E+04	
	WA1	18	1.85E+06	1.90E+06	
	WA2	7	1.22E+06	5.68E+05	
	WA3	7	1.11E+06	4.89E+05	
	WA4	6	1.17E+06	1.14E+05	
	WA5	13	1.21E+06	4.13E+05	
	WA6	5	2.42E+06	2.42E+06	
Ca	WA7	4	1.14E+06	4.81E+05	0.436
	Total	60	1.48E+06	1.31E+06	
	WA1	18	7.26E+04	5.76E+04	
	WA2	7	9.05E+04	1.67E+04	
	WA3	7	5.71E+04	1.43E+04	
	WA4	6	4.54E+04	6.48E+03	
	WA5	13	6.85E+04	1.51E+04	
	WA6	5	8.93E+04	9.78E+04	
Ti	WA7	4	8.23E+04	2.42E+04	0.511
	Total	60	7.13E+04	4.37E+04	
	WA1	18	4.60E+01	4.58E+01	
	WA2	7	5.95E+01	2.73E+01	
	WA3	7	1.91E+01	1.56E+01	
	WA4	6	5.87E+01	4.44E+01	
	WA5	13	1.89E+01	1.44E+01	
	WA6	5	1.05E+02	1.06E+02	
	WA7	4	4.09E+01	3.67E+01	

Appendix A (Continued)

Element	Region	N	Mean(ppb)	Std. Deviation	Sig.
Mn	Total	60	4.44E+01	4.81E+01	0.015
	WA1	18	7.80E+02	2.41E+02	
	WA2	7	8.71E+02	2.48E+02	
	WA3	7	6.76E+02	1.66E+02	
	WA4	6	6.05E+02	1.20E+02	
	WA5	13	6.83E+02	1.56E+02	
	WA6	5	8.40E+02	1.09E+02	
	WA7	4	7.24E+02	1.17E+02	
Fe	Total	60	7.41E+02	2.00E+02	0.139
	WA1	18	1.07E+03	5.21E+02	
	WA2	7	1.04E+03	1.04E+03	
	WA3	7	1.15E+03	3.45E+02	
	WA4	6	9.17E+02	3.61E+02	
	WA5	13	1.50E+03	1.20E+03	
	WA6	5	1.03E+03	3.58E+02	
	WA7	4	7.83E+02	4.17E+02	
Co	Total	60	1.13E+03	7.55E+02	0.593
	WA1	18	3.27E+00	1.07E+00	
	WA2	7	3.04E+00	1.77E+00	
	WA3	7	2.71E+00	8.24E-01	
	WA4	6	2.16E+00	7.41E-01	
	WA5	13	2.75E+00	8.80E-01	
	WA6	5	2.57E+00	1.12E+00	
	WA7	4	2.38E+00	5.36E-01	
Ni	Total	60	2.84E+00	1.07E+00	0.341
	WA1	18	1.46E+01	6.50E+00	
	WA2	7	2.66E+01	4.93E+00	
	WA3	7	1.16E+01	3.39E+00	
	WA4	6	9.30E+00	2.74E+00	
	WA5	13	1.38E+01	9.95E+00	
	WA6	5	1.37E+01	2.36E+00	
	WA7	4	1.56E+01	6.46E+00	
Cu	Total	60	1.49E+01	7.76E+00	0.001
	WA1	18	1.18E+02	9.93E+01	
	WA2	7	2.53E+01	2.07E+01	
	WA3	7	7.15E+01	6.72E+01	
	WA4	6	1.42E+02	1.06E+02	
	WA5	13	4.91E+01	2.82E+01	
	WA6	5	1.83E+02	9.62E+01	
	WA7	4	1.60E+02	1.56E+02	
	Total	60	9.75E+01	9.35E+01	0.007

Appendix A (Continued)

Element	Region	N	Mean(ppb)	Std. Deviation	Sig.
Zn	WA1	18	4.64E+02	2.17E+02	0.424
	WA2	7	2.85E+02	1.08E+02	
	WA3	7	4.79E+02	3.45E+02	
	WA4	6	3.61E+02	8.00E+01	
	WA5	13	4.40E+02	1.96E+02	
	WA6	5	3.66E+02	7.77E+01	
	WA7	4	3.40E+02	1.42E+02	
	Total	60	4.13E+02	2.02E+02	
As	WA1	18	2.91E+00	2.17E+00	0.261
	WA2	7	1.81E+00	1.64E+00	
	WA3	7	1.93E+00	7.85E-01	
	WA4	6	3.64E+00	1.87E+00	
	WA5	13	1.85E+00	1.41E+00	
	WA6	5	2.14E+00	7.78E-01	
	WA7	4	2.61E+00	1.35E+00	
	Total	60	2.43E+00	1.70E+00	
Rb	WA1	18	9.42E+02	3.80E+02	0.051
	WA2	7	6.27E+02	2.80E+02	
	WA3	7	5.56E+02	2.78E+02	
	WA4	6	5.82E+02	9.49E+01	
	WA5	13	6.77E+02	2.05E+02	
	WA6	5	7.45E+02	4.39E+02	
	WA7	4	7.07E+02	2.91E+02	
	Total	60	7.35E+02	3.25E+02	
Sr	WA1	18	7.52E+02	2.82E+02	0.564
	WA2	7	7.71E+02	1.56E+02	
	WA3	7	5.94E+02	1.16E+02	
	WA4	6	6.73E+02	1.23E+02	
	WA5	13	6.68E+02	1.31E+02	
	WA6	5	6.72E+02	1.69E+02	
	WA7	4	7.28E+02	1.40E+02	
	Total	60	7.02E+02	1.94E+02	
Y	WA1	18	4.14E-01	2.83E-01	0.1
	WA2	7	1.14E+00	7.18E-01	
	WA3	7	3.39E-01	1.99E-01	
	WA4	6	1.15E+00	2.11E+00	
	WA5	13	3.50E-01	2.17E-01	
	WA6	5	2.97E-01	1.50E-01	
	WA7	4	6.19E-01	5.64E-01	
	Total	60	5.53E-01	7.66E-01	
Zr	WA1	18	2.58E+01	2.36E+01	

Appendix A (Continued)

Element	Region	N	Mean(ppb)	Std. Deviation	Sig.		
Cs	WA2	7	1.24E+01	5.23E+00	0.015		
	WA3	7	8.35E+00	8.61E+00			
	WA4	6	1.83E+01	1.16E+01			
	WA5	13	8.23E+00	4.67E+00			
	WA6	5	3.45E+01	2.60E+01			
	WA7	4	1.46E+01	7.44E+00			
	Total	60	1.76E+01	1.77E+01			
	WA1	18	2.25E+00	1.44E+00			
	WA2	7	2.47E+00	3.35E+00			
	WA3	7	1.00E+00	6.09E-01			
Ba	WA4	6	1.10E+00	3.13E-01	0.568		
	WA5	13	1.60E+00	1.53E+00			
	WA6	5	1.99E+00	2.67E+00			
	WA7	4	1.70E+00	6.64E-01			
	Total	60	1.82E+00	1.74E+00			
	WA1	18	3.16E+02	1.04E+02			
	WA2	7	2.72E+02	6.17E+01			
	WA3	7	2.26E+02	6.13E+01			
	WA4	6	3.71E+02	8.78E+01			
	WA5	13	1.91E+02	6.88E+01			
La	WA6	5	4.65E+02	1.74E+02	0		
	WA7	4	3.18E+02	9.65E+01			
	Total	60	2.91E+02	1.19E+02			
	WA1	18	7.35E+00	7.59E+00			
	WA2	7	7.34E-01	3.89E-01			
	WA3	7	4.52E+00	5.57E+00			
	WA4	6	6.46E+00	7.16E+00			
	WA5	13	1.79E+00	4.11E+00			
	WA6	5	7.08E+00	6.60E+00			
	WA7	4	6.48E+00	7.40E+00			
Ce	Total	60	4.87E+00	6.34E+00	0.113		
	WA1	18	2.69E-01	2.47E-01			
	WA2	7	1.27E+00	1.09E+00			
	WA3	7	1.45E-01	1.50E-01			
	WA4	6	1.68E-01	1.27E-01			
	WA5	13	2.03E-01	1.33E-01			
	WA6	5	1.69E-01	8.84E-02			
	WA7	4	3.88E-01	3.50E-01			
	Pr	Total	60	3.46E-01		5.20E-01	0
		WA1	18	5.60E-02		9.30E-02	
WA2		7	1.61E-01	1.42E-01			

Appendix A (Continued)

Element	Region	N	Mean(ppb)	Std. Deviation	Sig.	
Nd	WA3	7	2.13E-02	1.97E-02		
	WA4	6	2.08E-02	1.26E-02		
	WA5	13	2.76E-02	1.91E-02		
	WA6	5	2.04E-02	1.27E-02		
	WA7	4	5.69E-02	5.28E-02		
	Total	60	5.16E-02	8.16E-02	0.007	
	WA1	18	2.33E-01	3.21E-01		
	WA2	7	7.13E-01	6.20E-01		
	WA3	7	8.92E-02	6.92E-02		
	WA4	6	8.88E-02	4.95E-02		
	WA5	13	1.15E-01	7.85E-02		
	WA6	5	1.08E-01	6.61E-02		
	WA7	4	2.55E-01	2.32E-01		
	Total	60	2.23E-01	3.32E-01	0.001	
Sm	WA1	18	3.85E-02	3.73E-02		
	WA2	7	1.93E-01	1.66E-01		
	WA3	7	2.22E-02	2.21E-02		
	WA4	6	1.87E-02	1.13E-02		
	WA5	13	3.30E-02	2.60E-02		
	WA6	5	2.22E-02	1.60E-02		
	WA7	4	6.19E-02	6.16E-02		
	Total	60	5.16E-02	7.99E-02	0	
	Eu	WA1	18	2.61E-02	1.30E-02	
		WA2	7	5.01E-02	3.40E-02	
		WA3	7	2.57E-02	4.92E-03	
		WA4	6	7.38E-02	1.24E-01	
		WA5	13	1.96E-02	5.12E-03	
		WA6	5	2.61E-02	9.87E-03	
WA7		4	3.29E-02	1.24E-02		
Total		60	3.27E-02	4.19E-02	0.168	
Gd		WA1	18	4.71E-02	4.45E-02	
		WA2	7	2.81E-01	1.67E-01	
		WA3	7	2.25E-02	1.88E-02	
		WA4	6	3.51E-02	2.52E-02	
		WA5	13	4.95E-02	4.00E-02	
		WA6	5	2.46E-02	1.60E-02	
	WA7	4	7.57E-02	7.67E-02		
	Total	60	7.09E-02	1.01E-01	0	
	Dy	WA1	18	4.76E-02	4.57E-02	
		WA2	7	2.20E-01	1.68E-01	
		WA3	7	2.44E-02	1.84E-02	

Appendix A (Continued)

Element	Region	N	Mean(ppb)	Std. Deviation	Sig.	
Ho	WA4	6	2.41E-02	8.60E-03		
	WA5	13	4.41E-02	3.81E-02		
	WA6	5	3.27E-02	2.19E-02		
	WA7	4	7.79E-02	8.21E-02		
	Total	60	6.26E-02	8.76E-02	0	
	WA1	18	1.27E-02	1.12E-02		
	WA2	7	4.69E-02	3.37E-02		
	WA3	7	7.60E-03	3.70E-03		
	WA4	6	6.49E-03	3.30E-03		
	WA5	13	1.12E-02	6.82E-03		
	WA6	5	8.99E-03	5.64E-03		
	WA7	4	2.25E-02	2.15E-02		
	Total	60	1.55E-02	1.83E-02	0	
	Er	WA1	18	3.81E-02	2.90E-02	
WA2		7	1.36E-01	8.89E-02		
WA3		7	3.51E-02	1.87E-02		
WA4		6	6.08E-02	7.90E-02		
WA5		13	3.78E-02	2.27E-02		
WA6		5	3.64E-02	1.64E-02		
WA7		4	8.03E-02	6.56E-02		
Total		60	5.41E-02	5.48E-02	0.001	
Tm		WA1	18	7.16E-03	4.13E-03	
		WA2	7	2.21E-02	1.23E-02	
		WA3	7	6.55E-03	2.45E-03	
		WA4	6	5.65E-03	2.09E-03	
		WA5	13	9.07E-03	3.74E-03	
		WA6	5	6.43E-03	3.62E-03	
	WA7	4	1.42E-02	1.18E-02		
	Total	60	9.50E-03	7.58E-03	0	
	Yb	WA1	18	6.05E-02	2.60E-02	
		WA2	7	1.46E-01	8.15E-02	
		WA3	7	3.88E-02	2.79E-02	
		WA4	6	2.17E-02	2.47E-02	
		WA5	13	5.83E-02	3.25E-02	
		WA6	5	4.32E-02	4.35E-02	
WA7		4	1.12E-01	9.73E-02		
Total		60	6.56E-02	5.56E-02	0	
Re		WA1	18	4.03E-02	2.47E-02	
		WA2	7	2.53E-02	1.82E-02	
		WA3	7	2.14E-02	8.17E-03	
		WA4	6	7.53E-02	6.73E-02	

Appendix A (Continued)

Element	Region	N	Mean(ppb)	Std. Deviation	Sig.		
Hg	WA5	13	8.65E-02	3.54E-02	0		
	WA6	5	4.23E-02	2.83E-02			
	WA7	4	4.30E-02	4.45E-02			
	Total	60	5.02E-02	3.97E-02			
	WA1	18	1.06E-01	8.07E-02			
	WA2	7	8.62E-02	6.69E-03			
	WA3	7	7.37E-02	4.35E-02			
	WA4	6	1.47E-01	1.66E-01			
	WA5	13	8.52E-02	4.94E-02			
	WA6	5	6.93E-02	6.03E-02			
Pb	WA7	4	2.20E-01	1.51E-01	0.081		
	Total	60	1.04E-01	8.80E-02			
	WA1	18	4.46E+00	3.20E+00			
	WA2	7	1.05E+01	6.67E+00			
	WA3	7	3.56E+00	1.98E+00			
	WA4	6	2.63E+00	1.62E+00			
	WA5	13	6.05E+00	7.83E+00			
	WA6	5	2.47E+00	6.02E-01			
	WA7	4	5.82E+00	4.69E+00			
	Total	60	5.15E+00	5.20E+00			
Th	WA1	18	1.31E-01	7.18E-02	0.061		
	WA2	7	6.28E-01	5.67E-01			
	WA3	7	1.26E-01	9.71E-02			
	WA4	6	1.31E-01	5.75E-02			
	WA5	13	2.44E-01	1.34E-01			
	WA6	5	1.95E-01	1.14E-01			
	WA7	4	2.51E-01	7.03E-02			
	Total	60	2.26E-01	2.54E-01			
	Delta O 18	WA1	18	2.20E+00		1.74E+00	0
		WA2	7	1.41E+00		2.58E+00	
WA3		7	-3.58E-01	2.13E+00			
WA4		6	2.26E+00	7.59E-01			
WA5		13	-3.06E-01	2.32E+00			
WA6		5	2.44E+00	1.75E+00			
WA7		4	-4.83E-01	2.42E+00			
Total		60	1.11E+00	2.28E+00			
Delta D		WA1	18	-3.60E+01	1.52E+01	0.004	
		WA2	7	-3.79E+01	1.35E+01		
	WA3	7	-5.20E+01	7.34E+00			
	WA4	6	-3.75E+01	8.36E+00			
	WA5	13	-5.04E+01	1.16E+01			

Appendix A (Continued)

Element	Region	N	Mean(ppb)	Std. Deviation	Sig.
	WA6	5	-3.52E+01	6.44E+00	
	WA7	4	-5.45E+01	1.35E+01	
	Total	60	-4.25E+01	1.39E+01	0.004

Appendix B-PCA factor loadings for wines from WA regions.

Variables	Principal Components										
	PC 1	PC 2	PC 3	PC 4	PC 5	PC 6	PC 7	PC 8	PC 9	PC 10	PC 11
%											
Variance	19.98	8.02	6.84	6.44	5.86	5.76	5.4	4.04	3.88	3.83	3.63
Li	-0.116	-0.08	0.069	-0.253	0.103	0.509	0.511	0.203	-0.02	0.396	-0.026
Be	-0.055	0.627	-0.362	0.057	-0.027	0.172	0.006	0	0.054	-0.097	-0.441
B	-0.128	-0.155	0.43	0.194	0.027	0.212	0.049	0.419	-0.042	0.13	0.53
Na	0.155	-0.054	-0.004	-0.003	-0.1	0.172	-0.154	0.871	0.032	-0.004	0.008
Mg	0.11	-0.046	0.107	0.935	-0.032	0.043	-0.094	-0.026	-0.078	-0.084	0.086
Al	0.309	0.853	-0.071	0.164	0.082	0.036	0.132	0.08	0.13	-0.005	0.006
Si	0.215	0.172	0.383	0.396	-0.245	-0.182	-0.026	0.262	-0.323	-0.227	0.276
P	-0.145	0.012	0.289	0.435	-0.078	-0.027	0.061	0.102	0.222	0.116	0.689
S	0.048	-0.107	0.51	0.185	-0.025	-0.331	-0.235	0.122	0.311	-0.096	-0.1
K	-0.017	-0.115	0.197	0.924	-0.026	-0.008	-0.115	0.037	-0.001	-0.056	0.151
Ca	-0.045	0.178	0.004	0.944	-0.045	0.035	-0.051	-0.053	-0.064	-0.012	-0.131
Ti	-0.091	0.201	0.187	0.548	0.165	-0.077	-0.058	0.076	0.39	-0.169	0.305
V	0.271	0.732	0.385	0.078	0.015	0.022	-0.098	-0.006	-0.136	0.026	-0.053
Mn	0.122	0.161	0.805	0.213	0.044	0.115	0.097	0.281	0.027	0.016	0.02
Fe	0.16	0.721	-0.238	-0.124	-0.034	-0.004	-0.001	-0.034	-0.123	-0.124	0.371
Co	0.082	0.411	-0.069	0.031	-0.19	0.422	0.438	-0.13	-0.057	-0.227	0.168
Ni	0.175	-0.022	0.211	0.23	-0.076	0	0.053	0.063	-0.06	0.042	0.153
Cu	0.123	-0.092	0.067	-0.221	-0.119	0.218	0.471	0.184	-0.016	-0.143	0.503
Zn	0.318	0.182	-0.16	-0.084	-0.031	0.368	-0.058	-0.318	-0.035	-0.122	-0.13
Ga	0.2	0.875	0.002	0.04	0.145	-0.129	0.029	-0.16	-0.023	-0.199	-0.07
As	0.267	0.395	0.088	0.265	0.036	0.059	0.129	0.129	0.017	0.103	0.06
Se	0.049	0.048	0.133	0.253	0.014	-0.055	0.267	0.552	0.129	-0.075	0.241
Rb	0.123	0.111	0.778	0.044	-0.034	0.018	0.117	-0.103	0.016	-0.105	0.174
Sr	0.239	0.182	0.73	-0.008	0.048	0.25	-0.13	-0.03	-0.117	0.021	0.351
Y	0.832	0.18	0.102	0.083	0.041	0.211	-0.039	0.102	0.064	0.019	0.123
Zr	0.053	0.061	0.178	-0.112	0.048	0.055	0.896	-0.013	0.062	0.088	0.23
Mo	0.27	0.121	0.185	-0.118	0.002	0.194	0.073	0.783	-0.125	0.132	0.094
Pd	0.02	0.021	-0.018	0.019	0	-0.268	-0.059	0.019	0.72	-0.206	0.117
Ag	-0.043	0.038	0.016	0.404	-0.171	-0.541	-0.082	-0.355	-0.061	-0.383	-0.107
Cd	0.14	0.388	0.186	0.406	-0.048	-0.104	-0.089	0.048	0.03	-0.291	-0.231
Sn	0.119	-0.101	-0.216	0.025	0.478	-0.048	-0.068	-0.063	0	-0.122	0.01
Sb	0.177	0.875	0.154	-0.041	0.055	0.012	0.011	-0.019	-0.133	0.067	-0.034
Cs	0.144	0.713	0.494	-0.035	0.072	0.021	0.055	-0.023	-0.031	-0.133	0.02
Ba	0.029	0.097	0.313	0.092	0.199	0.256	0.308	0.058	0.179	0.144	0.58
La	-0.122	-0.026	0.045	-0.144	0.125	0.218	0.786	-0.068	-0.044	0.245	-0.152
Ce	0.86	0.222	0.324	0.05	0.133	0.011	-0.001	0.078	0.017	-0.034	-0.063
Pr	0.199	0.064	0.135	-0.036	0.94	0.064	0.036	-0.015	-0.026	-0.005	0.001
Nd	0.266	0.083	0.148	-0.048	0.917	0.094	0.088	-0.035	-0.04	0.017	-0.013
Sm	0.904	0.221	0.14	-0.027	0.174	0.039	0.034	0.046	-0.053	0.033	-0.085
Eu	0.417	0.246	0.349	-0.154	0.058	0.476	0.122	0.12	0.045	0.295	0.217
Gd	0.854	0.124	0.049	-0.005	0.126	-0.145	0.202	0.028	0.042	-0.036	0.002

Appendix B (Continued)

Variables	PC 1	PC 2	PC 3	PC 4	PC 5	PC 6	PC 7	PC 8	PC 9	PC 10	PC 11
%											
Variance	19.98	8.02	6.84	6.44	5.86	5.76	5.4	4.04	3.88	3.83	3.63
Dy	0.774	0.08	-0.033	0.001	0.599	-0.035	-0.028	-0.014	0.04	-0.07	0.052
Ho	0.594	0.083	-0.013	-0.047	0.771	-0.04	0.005	-0.025	-0.003	-0.032	0.003
Er	0.892	0.165	-0.051	-0.018	0.135	0.027	-0.09	0.148	0.047	-0.028	0.032
Tm	0.774	0.275	-0.075	-0.139	0.11	-0.062	-0.135	0.032	-0.034	0.005	-0.05
Yb	0.51	0.404	-0.072	0.002	0.246	0.04	0.15	-0.041	-0.055	0.026	-0.169
Hf	0.096	-0.147	-0.116	-0.162	-0.033	0.071	0.001	0.391	0.131	0.794	0.114
Ta	0.134	-0.032	-0.063	-0.08	-0.05	-0.072	-0.081	0.004	0.928	0.033	0.071
W	0.106	0.898	-0.072	-0.023	-0.026	-0.114	-0.072	0.126	0.037	0.068	0.066
Re	-0.09	-0.033	0.158	-0.162	-0.089	-0.589	-0.181	-0.237	-0.003	-0.191	-0.07
Ir	-0.073	-0.143	0.138	-0.031	-0.028	0.279	0.25	-0.052	0.767	0.307	-0.037
Pt	0.031	0.117	-0.12	-0.354	-0.026	-0.273	0.257	-0.12	-0.215	0.202	-0.087
Au	-0.082	-0.044	-0.091	-0.054	-0.048	-0.06	0.186	-0.127	0.014	0.892	0.005
Hg	-0.098	-0.084	-0.01	-0.122	0.119	0.025	0.178	-0.089	0.195	-0.02	-0.073
Tl	0.367	0.375	0.521	0.122	0.046	-0.297	0.046	0.113	0.107	-0.09	-0.133
Pb	0.171	0.391	-0.23	-0.033	0.037	0.045	-0.023	-0.073	-0.012	-0.095	-0.135
Th	0.029	0.158	-0.071	-0.123	-0.055	-0.749	-0.173	-0.216	0.047	0.14	-0.053
U	0.711	-0.062	0.181	0.217	-0.042	0.013	-0.118	0.111	-0.014	-0.006	0.055
Delta O 18	0.067	-0.341	0.696	0.227	0.164	-0.035	0.205	0.077	0.089	-0.056	0.23
Delta D	-0.036	-0.15	0.698	0.11	0.196	-0.128	0.178	0.012	-0.026	-0.121	-0.042